

**GEOPHYSICAL INVESTIGATION
OF A DIABASE DIKE**

A THESIS

Presented to

**The Faculty of the Division of Graduate
Studies and Research**

by

George Henry Rothe, III

**In Partial Fulfillment
of the Requirements for the Degree
Master of Science in Geophysical Sciences**

Georgia Institute of Technology

November, 1973

GEOPHYSICAL INVESTIGATION OF A DIABASE DIKE

Approved:

Chairman

Date approved by Chairman:

11-28-73

ACKNOWLEDGEMENTS

The author wishes to express his gratitude to Dr. L. Timothy Long for his guidance in this study and to Drs. G. Lafayette Maynard and J. Marion Wampler for their suggestions and for reviewing this manuscript. Thanks to Dr. Robert Bentley for his helpful discussions concerning the geology of the Georgia Piedmont. Thanks to Mr. Doyle Watts of the Ohio State University for supplying the paleomagnetic data for the Meriwether dike.

During my tenure as a graduate student I received support in part through a research assistantship made possible by grant #DA-ARO-D-31-124-71-G117 from the Army Research Office - Durham. Also, my thesis research was supported in part by this grant. This support is appreciated.

The School of Geophysical Sciences provided the computer time for the analysis of the data.

Special thanks to Mr. Roland Schenck who assisted in collecting the data. And special thanks to my wife, Donna, for her assistance in the collecting of data, and for editing and typing this manuscript.

TABLE OF CONTENTS

	Page
ACKNOWLEDGEMENTS	ii
LIST OF TABLES	v
LIST OF FIGURES	vi
SUMMARY	viii
Chapter	
I. INTRODUCTION	1
II. GEOLOGIC SETTING AND REGIONAL GEOPHYSICS	6
Geologic Setting	
Regional Gravity	
Regional Magnetics	
III. PHYSICAL PROPERTIES OF THE MERIWETHER DIKE	16
Density	
Magnetic Susceptibility	
IV. DETERMINATION OF DIP ANGLE FROM GRAVITY AND MAGNETIC ANOMALIES	18
Theoretical Models	
Detailed Gravity Profiles	
V. GROUND-LEVEL MAGNETICS AND THE ROLE OF NATURAL REMANENT MAGNETIZATION IN THE OBSERVED ANOMALIES	30
Ground-Level Magnetics	
Natural Remanent Magnetization of the Meriwether Dike	
Theoretical Anomalies and the Determination of the Koenigsberger Ratio, Q	
VI. DISCUSSION AND CONCLUSIONS	35
APPENDICES	37
I. Gravity Surveys and Data Reduction	
II. Ground-Level Magnetic Surveys and Data Reduction	

Table of Contents (Concluded)

	Page
III. Computer Programs for Gravity and Magnetic Modeling	
IV. Paleomagnetic Data Collection and Reduction	
BIBLIOGRAPHY	75

LIST OF TABLES

Table	Page
1. Gravity Base Stations Used in this Study	39
2. Instrumental Drift for Worden Gravimeter	39
3. Gravity Data	42
4. Ground-Level Magnetics Data	51
5. Two-Dimensional Gravity Modeling Program	61
6. Two-Dimensional Magnetics Modeling Program	63
7. Natural Remanent Moments of Cores Taken from the Meriwether Dike	74

LIST OF FIGURES

Figure	Page
1. Map of Diabase Dikes in Eastern North America, West Africa, and Northeastern South America with the Continents Restored to Their Relative Position in the Triassic	2
2. Geology of the Inner Piedmont of West Georgia	5
3. Geology of the Inner Piedmont of West Georgia	7
4. Simple Bouguer Gravity Map of Detail Study Area	8
5. Index Map of Georgia Showing Location of Detail Study Area and Existing Aeromagnetic Maps	10
6. Portion of North-Central Georgia Aeromagnetic Map Covering Area of Detail Study	11
7. Index Map Showing Locations of Detailed Ground-Level Magnetic Surveys and Existing Aeromagnetic Flight Lines	13
8. Ground-Level Magnetic Profiles	14
9. Aeromagnetic Map of the Study Area Recontoured Assuming the Meriwether Dike to be a Continuous Magnetic Feature	15
10. Calculated Curves Showing Effect of Dip Angle on Vertical Gravity Anomaly	19
11. Calculated Curves Showing Effect of Dip Angle on Total Field Anomaly Due to Induction Magnetization Only	20
12. Detailed Gravity Profile A-A'	22
13. Detailed Gravity Profile B-B'	23
14. Detailed Gravity Profile C-C'	24
15. Detailed Gravity Profile D-D'	25
16. Detailed Gravity Profile E-E'	26

List of Figures (Concluded)

Figure	Page
17. Stereographic Projection of Measured Natural Remanent Moments for the Meriwether Dike	32
18. Calculated Curves Showing the Effect of Natural Remanent Magnetism on the Observed Total Field Anomaly	33
19. Standard Department of Defense Gravity Coding Form . .	41
20. Magnetogram for May 5, 1973	49
21. Magnetogram for May 6, 1973	50

SUMMARY

Analysis of gravity, aeromagnetic, ground-level magnetic, paleomagnetic, and high altitude infrared data has revealed a complex injection zone of diabase in central Meriwether County, Georgia. This zone, which previously was considered to be a single large (30-40 meters wide) diabase dike, has been found in places to reach a width of one kilometer.

A simple Bouguer gravity map of the area shows the dikes, which compose the injection zone, to be responsible for an anomaly in the regional gravity trend of about one to two milligals. Combined results from five gravity and three total-field magnetic traverses has suggested the dikes to dip at about 70° toward $N70^{\circ}E$. The mean of the observed ground-level magnetic anomalies for the dikes is a 1000 γ positive anomaly (total field).

On the basis of observed paleomagnetic data and computed bulk susceptibilities the ratio of the remanent to induced magnetizations (Koenigsberger's ratio, Q) has been calculated to be between 0.25 and 0.5. However, the shapes of the observed ground-level magnetic anomalies suggests a Q value of 1.0 or slightly higher for the Meriwether dike.

The total-field magnetic map based on already existing aeromagnetic data has been recontoured under the assumption that the Meriwether dike is continuous, as suggested by ground-level data taken during this investigation.

On the recontoured map the dike is the most prominent magnetic

feature of the area which suggests that the spacing and direction of the aeromagnetic flight lines is inappropriate for correlating dike caused anomalies of limited extent, even though the dike anomalies are large in magnitude.

High altitude infrared photographs show a change in intensity of reflected infrared radiation from vegetation growing on diabase derived soils suggesting that such pictures can be used to map the outcrop pattern of the dike in heavily wooded, highly weathered, and other inaccessible areas. It is suggested that this technique be applied to other areas of eastern North America to determine outcrop patterns of the dikes in areas not yet geologically mapped.

CHAPTER I

INTRODUCTION

A system of diabase dike swarms outcrops throughout eastern North America from Alabama to Nova Scotia (Cohee, et al., 1962), (Stockwell, et al., 1969). Southward along the Appalachian belt from Nova Scotia through New England and into the southern Piedmont, a gradual systematic change in strike is evident (Figure 1). King (1961) commented that the pattern of diabase dikes in eastern North America is probably the result of deep-seated stresses, but that the cause of the stresses is not apparent. May (1971) noted that the systematic pattern of the dikes in eastern North America is actually part of a larger, radial, pattern of diabase dikes surrounding the North Atlantic (Figure 1) and suggested that this pattern is a result of the stress field associated with the onset of North Atlantic sea-floor spreading in Late Triassic or Early Jurassic time.

The age of the dikes in eastern North America is currently in dispute. On the basis of fossil pole positions, de Boer (1967) suggested a Jurassic age for the dikes. On the other hand, Armstrong and Besancon (1970) found whole rock K-Ar ages to fall into two clusters: one at about 200 million years (Middle Triassic) and another smaller one between 225 and 230 million years (Early Triassic). Armstrong and Besancon (1970) suggested that the older dates may represent the actual time of emplacement, while the younger group may be indicative of "burial"

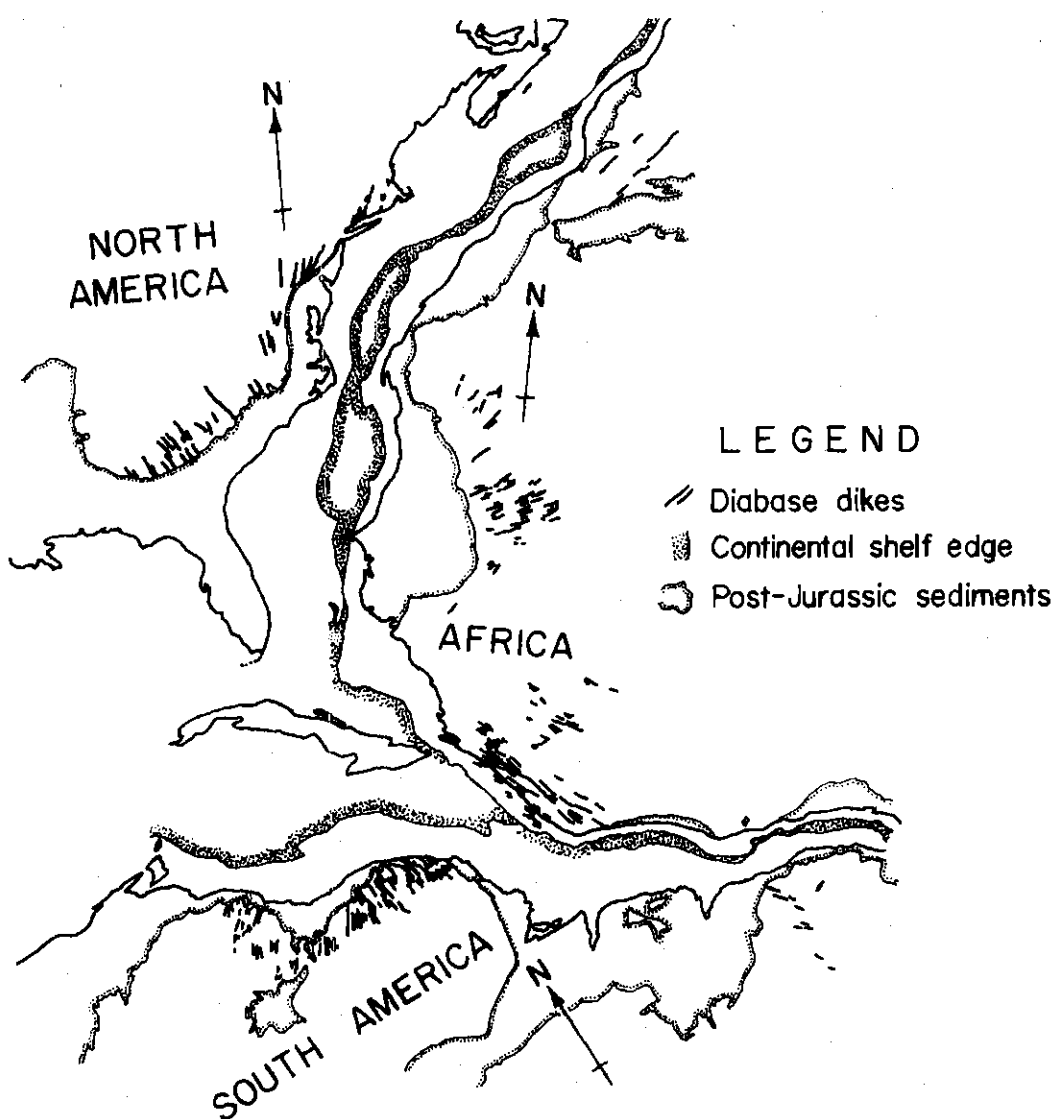


Figure 1. Map of Diabase Dikes in Eastern North America, West Africa, and Northeastern South America with the Continents Restored to Their Relative Position in the Triassic (after May, 1971). (North arrows indicate present geographic direction for each continent.)

metamorphism.

The chemistry of the diabase dikes, previously thought to be uniform (Lester and Allen, 1950) has been shown by Weigand and Ragland (1970) to vary in both major and trace element assemblages. Weigand and Ragland (1970) divided the dikes of eastern North America into several provinces based on the occurrence of three main chemical types: (1) olivine-normative, (2) high-TiO₂, quartz-normative and (3) low-TiO₂, quartz-normative.

The tracing of individual dikes along strike and the determination of thickness and dip by the usual geological field methods is inhibited in most areas of Southeastern North America by intense chemical weathering and dense vegetation. However, Johnson and Watkins (1963) noted a coincidence of dike outcrops and low-amplitude (less than 20 γ at an altitude of 800 feet above ground level), positive magnetic anomalies along aeromagnetic flight lines in north-central Virginia. On the basis of linear trends in the occurrence of some of these magnetic highs, Johnson and Watkins (1963) inferred the extension of dikes into areas where no outcrops are known. The success of Johnson and Watkins (1963) suggests that geophysical methods at closer range, i.e. aeromagnetics at 500 feet, ground-level magnetics and detailed gravity, could yield detailed structural information as well as outcrop patterns. The purpose of this study was to apply these geophysical methods to a study of the structure of a diabase dike.

A portion of the long dike in central Meriwether County in west-central Georgia (hereinafter referred to as the Meriwether dike) was selected for study. The dike extends southward from an area north-east

of Newnan in Coweta County, to an area south of the Towaliga fault in southern Meriwether county (Figure 2). This area of study was selected because of minimal secondary geophysical disturbances, such as gravity and magnetic anomalies associated with fault zones and basic intrusives other than the diabase dike. In addition, the roads in this area traverse the Meriwether dike at almost right angles and are spaced at approximately two miles, affording good access for a geophysical study.

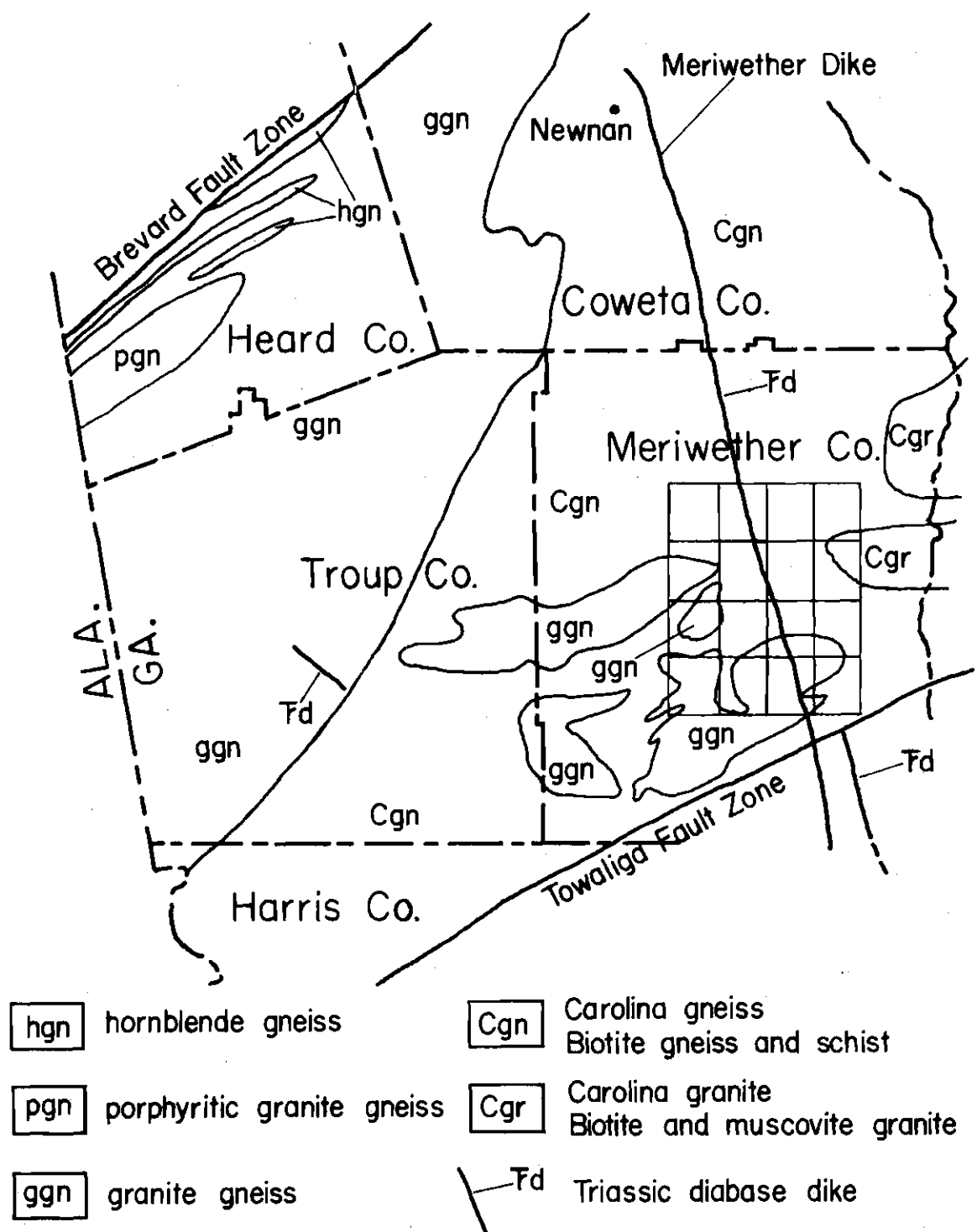


Figure 2. Geology of the Inner Piedmont of West Georgia (after the 1939 Geologic Map of Georgia). (Hatched square grid shows area of detail study.)

CHAPTER II

GEOLOGICAL SETTING AND REGIONAL GEOPHYSICS

Geologic Setting

According to the Geologic Map of the State of Georgia (Georgia Department of Mines, Mining and Geology, 1939) the geologic formations of the study area consist of granites intermingled with both biotite and granite gneisses (Figure 2). Recent reconnaissance mapping by R. D. Bentley (personal communications) has revealed the geology of the Inner Piedmont (between the Brevard and Towliga Fault Zones) to be more complicated than suggested by the 1939 Georgia Geology Map. Bentley and Neathery (1970) renamed the rocks of the southeastern portion of the Inner Piedmont the Opelika Complex and divided it into two stratigraphic units, the Loachapoka Schist and the Auburn Gneiss-schist (Figure 3). These units were interpreted by Bentley (Bentley and Neathery, 1970) as metamorphosed sediments which are extensively intermingled with granites. The Meriwether dike strikes about N 20° W through the area and intersects the rocks of the Opelika Complex at about 60°.

Regional Gravity

Based on measurements taken at 195 stations, a simple Bouguer gravity map of the area under investigation was constructed (Figure 4). The procedures used for the reduction of the data and estimating errors in the final values are given in Appendix I. Estimated error in the regional data is ± 0.35 milligals. Isogals trend approximately north-

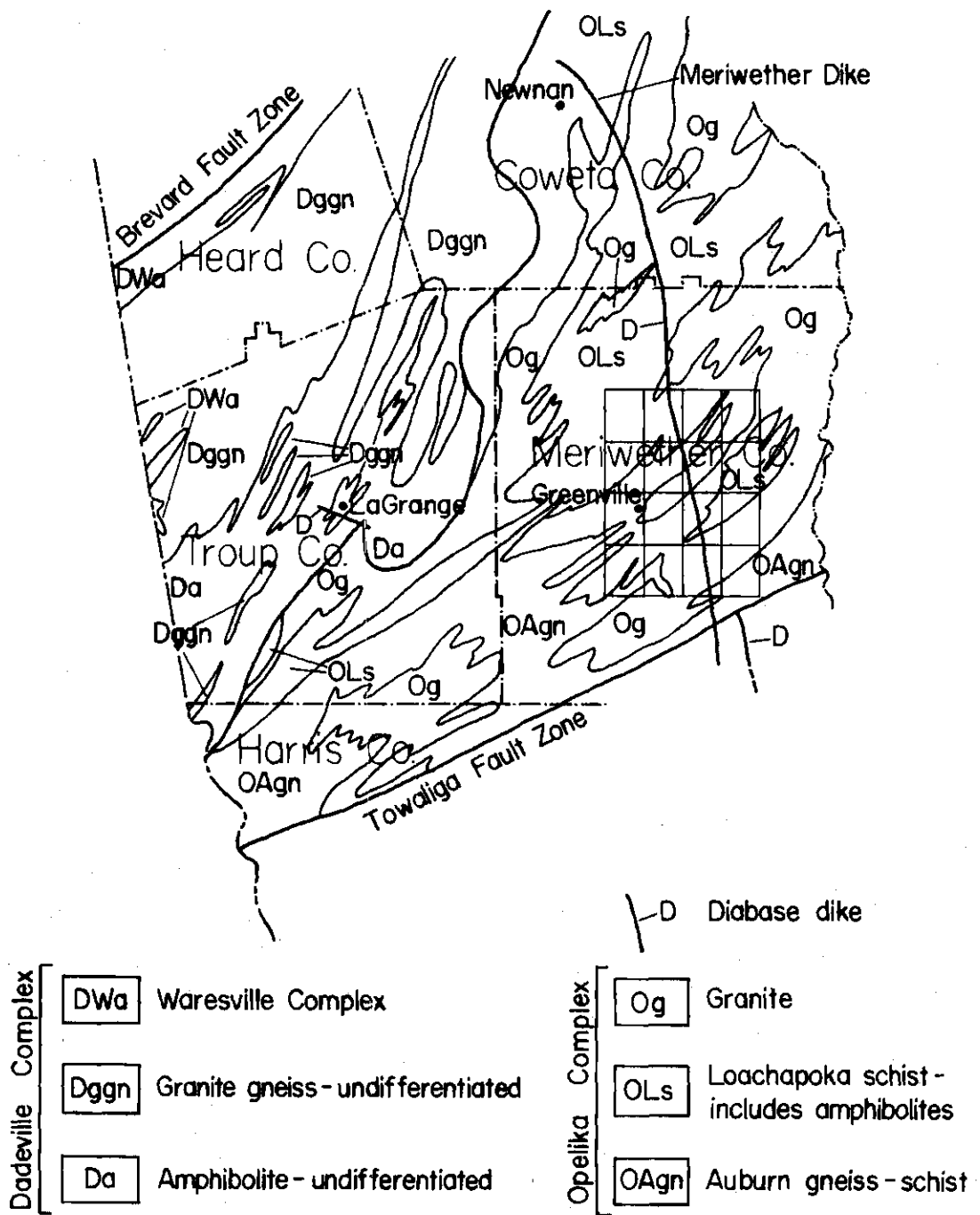


Figure 3. Geology of the Inner Piedmont of West Georgia (after Bentley Neathery, 1970). (Hatched square grid shows area of detail study.)

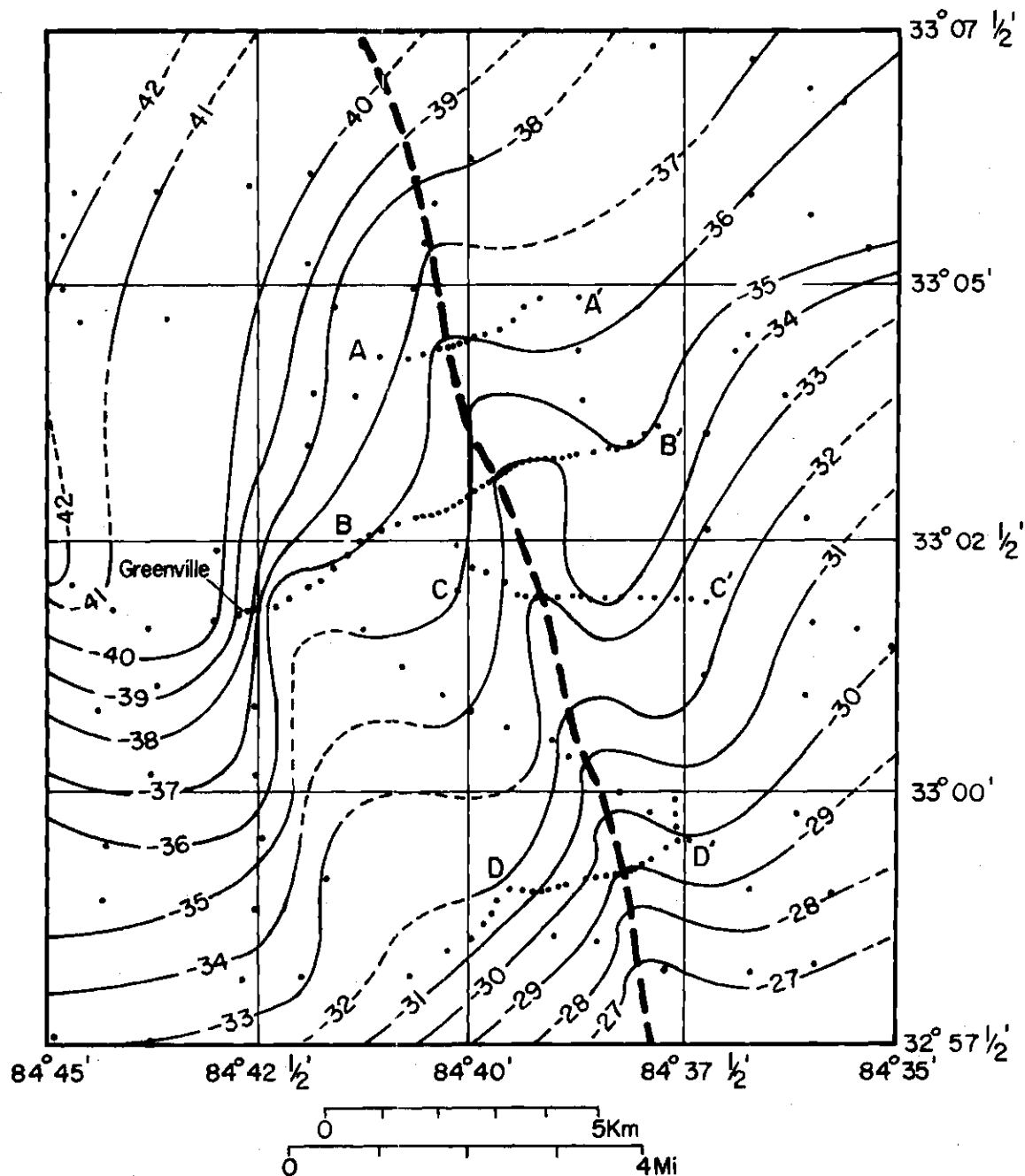


Figure 4. Simple Bouguer Gravity Map of Detail Study Area. (Dashed line gives location of Meriwether dike. Letters designate beginning and end of detailed gravity lines.)

east-southwest, and the regional gradient is about -0.8 milligals/kilometer to the northwest. The prominent features on the simple Bouguer gravity map are the steep gradient in the west-central portion of the study area and an anomaly in the regional trend of one to two milligals beginning in the southeastern part of the study area and continuing northward through the area. The steep gradient is coincidental with the contact between the Loachapoka Schist and granite west of Greenville (Figure 3). The anomaly in the regional trend is largely caused by the existence of the Meriwether dike. Too few gravity stations were taken in the extreme northern portion of the study area to warrant contouring, except by extrapolation. The anomaly probably extends northward out of the study area coincident with the dike.

Regional Magnetics

The North-Central Georgia Aeromagnetics Map (U.S. Geological Survey, open file, 1973) partially fills the gap (Figure 5) between the two previous aeromagnetic surveys of North Georgia Nuclear Laboratory (Philbin, Petrafeso and Long, 1964) and Savannah River Plant (Petty, Petrafeso and Moore, 1965). The area of this investigation (Figure 6) is part of the area covered by this latest work.

Similar to the regional gravity, magnetic features trend NE-SW. Lack of steep gradient immediately east of Greenville suggests that the units responsible for the observed steep gravity gradient in this area have a low contrast in magnetic susceptibility. The most conspicuous feature is the string of localized magnetic highs trending from north to south and having centers located at intersections of the dike and the

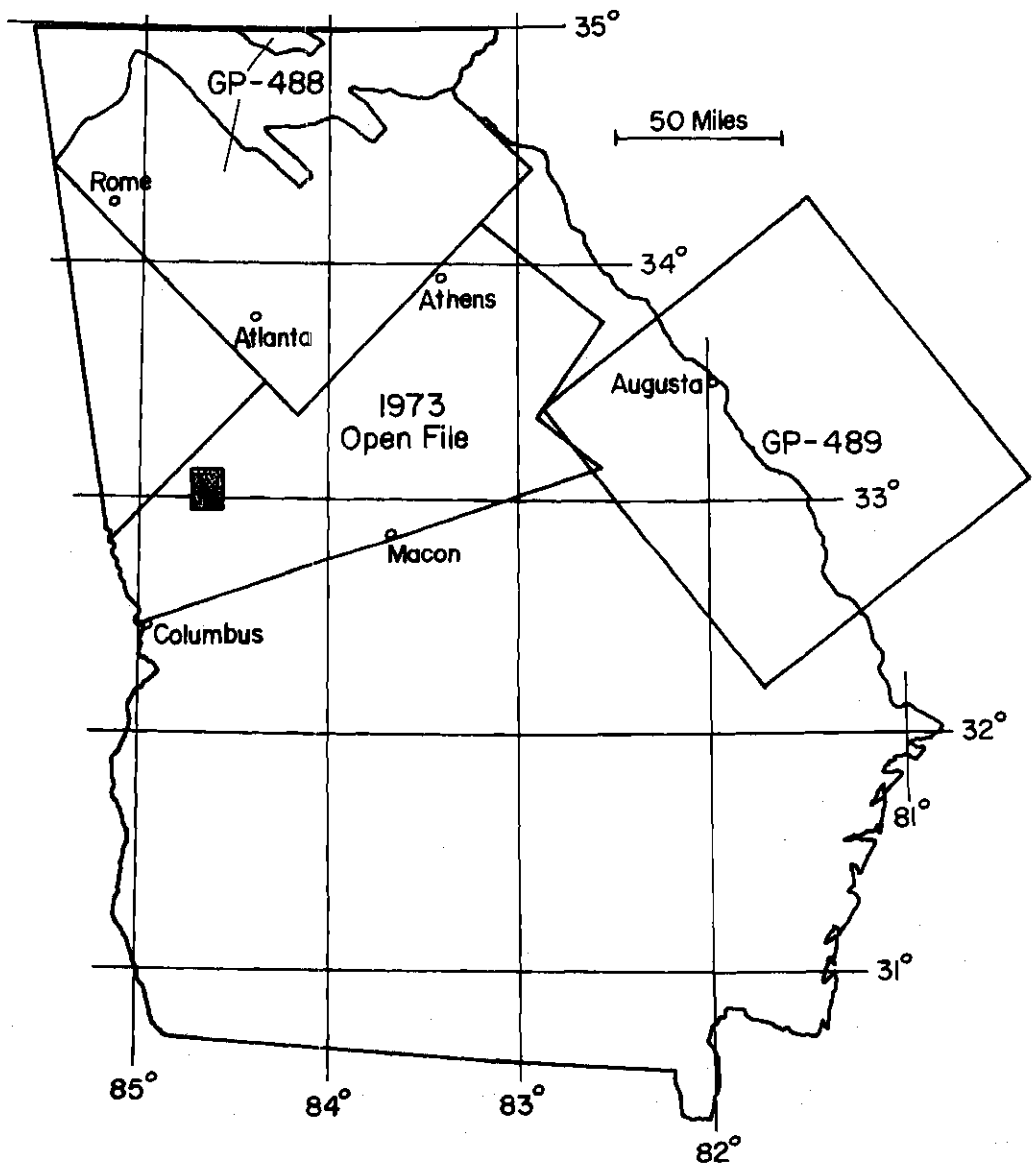


Figure 5. Index Map of Georgia Showing Location of Detail Study Area and Existing Aeromagnetic Maps. (Maps GP-488, North Georgia Nuclear Laboratory, and GP-489, Savannah River Plant, have been published by the U. S. Geological Survey. The North-Central Georgia Map is available on open file at the Georgia Geological Survey. Stippled rectangle is area of detail study.)

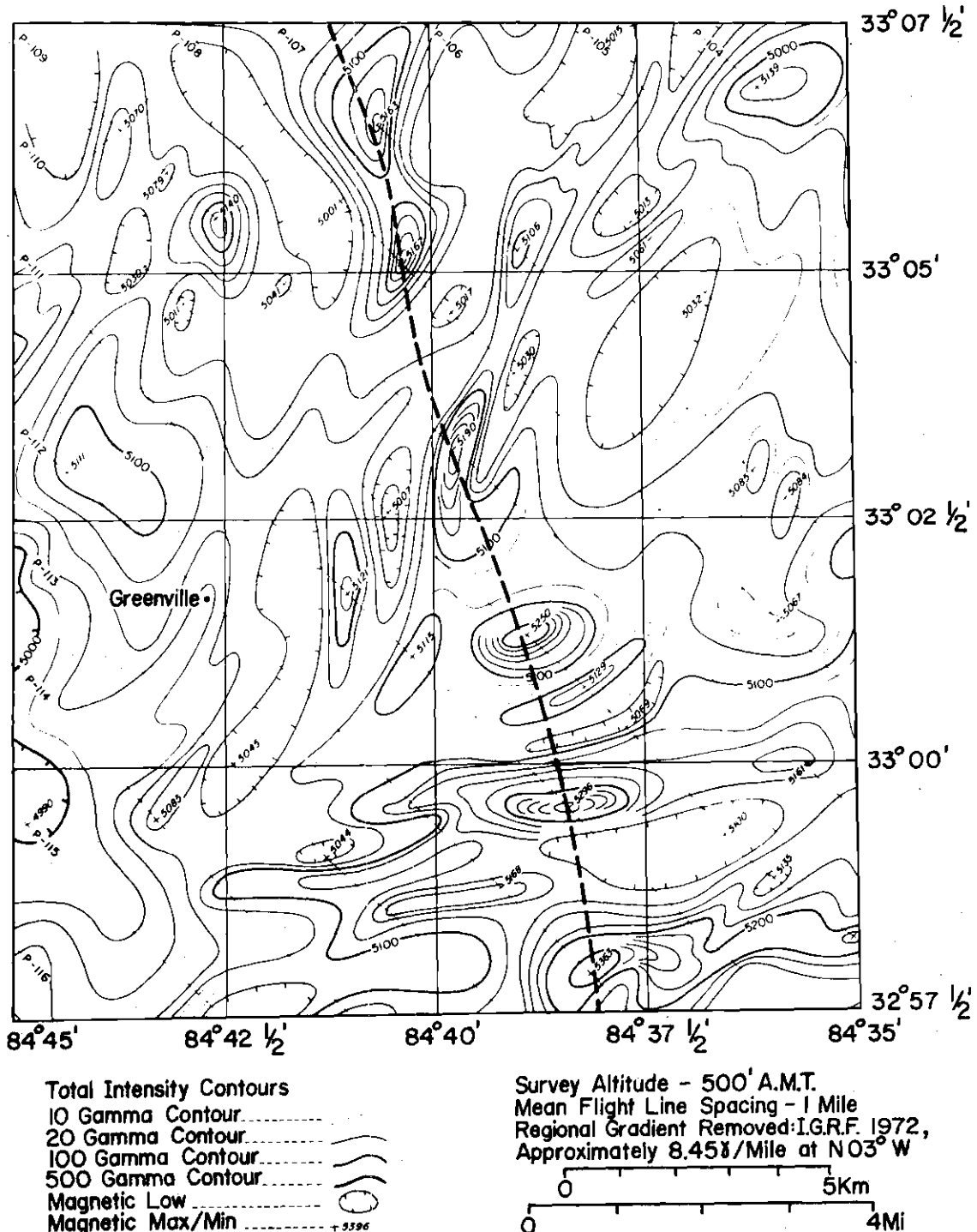


Figure 6. Portion of North-Central Georgia Aeromagnetic Map Covering Area of Detail Study. (U.S.G.S. Open File, 1973) (Dashed line gives location of Meriwether dike. Anomalies are with reference to 50,000' datum.)

flight lines. These magnetic highs are probably a result of the presence of the Meriwether dike.

The Meriwether dike, which outcrops on roads along its entire length, is probably more continuous than suggested by the series of magnetic highs in Figure 6. Detailed ground-level magnetic traverses of the Meriwether dike at points between aeromagnetic flight lines (Figure 7) support this supposition of continuity. Prominent (1000%) magnetic highs coinciding with observed dike outcroppings (Figure 8) suggested a recontouring of the aeromagnetic data.

Since the continuous flight line data were not available, all points where flight lines intersect contour lines were assumed to represent true values (the data were extrapolated by computer methods between flight lines). Latitude, longitude, and the total magnetic intensity were determined for each intersection and these points were plotted for recontouring. Under the assumption that the Meriwether dike is continuous along strike, straight lines were drawn connecting points of equal total magnetic intensity on adjacent flight lines in the region where the dike outcrops. In other areas contour lines were assumed to be influenced by the regional geology (after Bentley and Neathery, 1970).

Although no magnetic interpretation is unique, this one (Figure 9) does strongly suggest that the magnetic anomalies associated with the dike can be represented by a continuous linear anomaly. This interpretation is necessary for two-dimensional analysis of the dike by comparison of its observed anomalies with those of easily computed models.

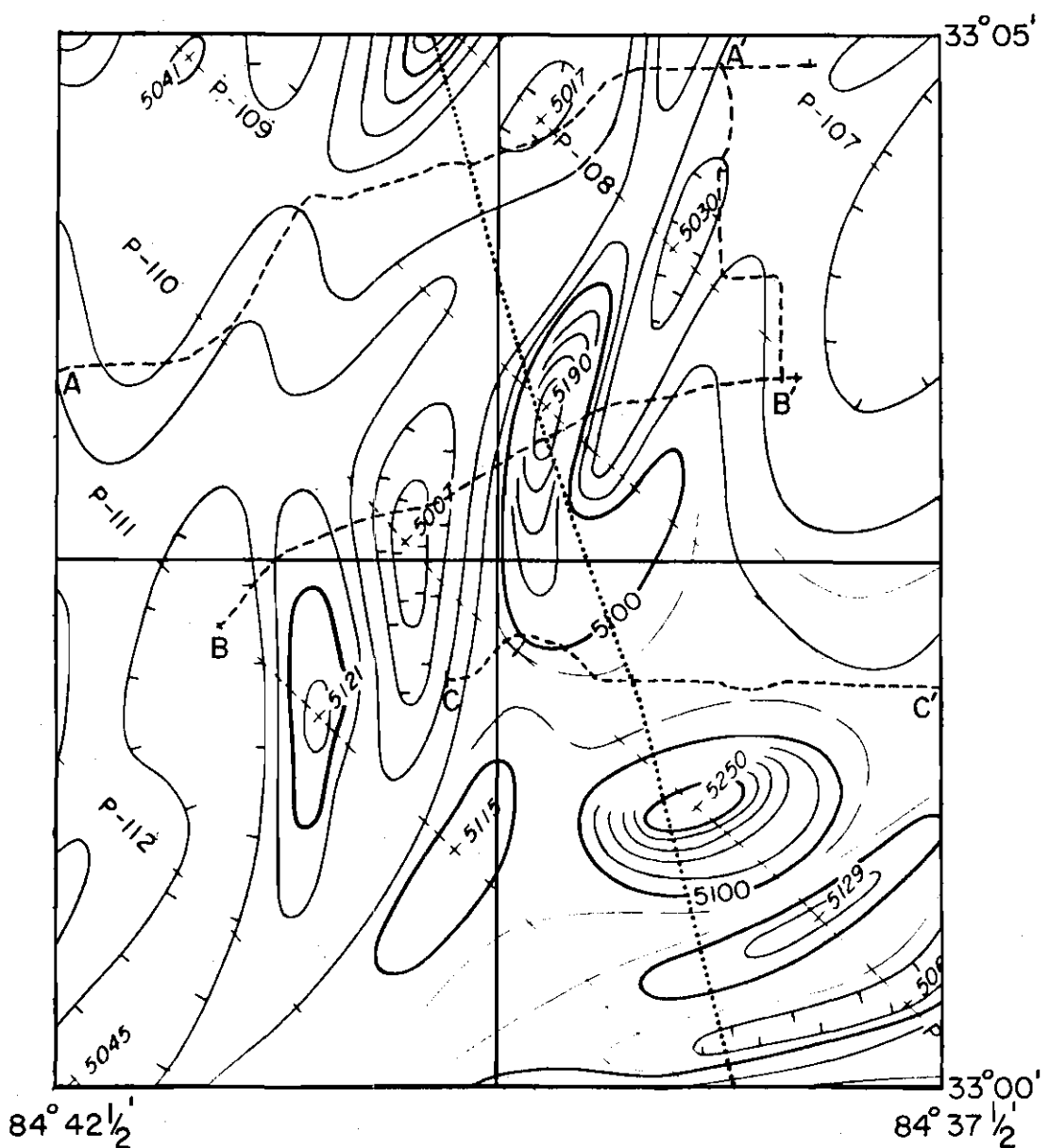


Figure 7. Index Map Showing Locations of Detailed Ground-Level Magnetic Surveys and Existing Aeromagnetic Flight Lines. (Dotted line gives location of Meriwether dike. Anomalies are with reference to 50,000 γ datum.)

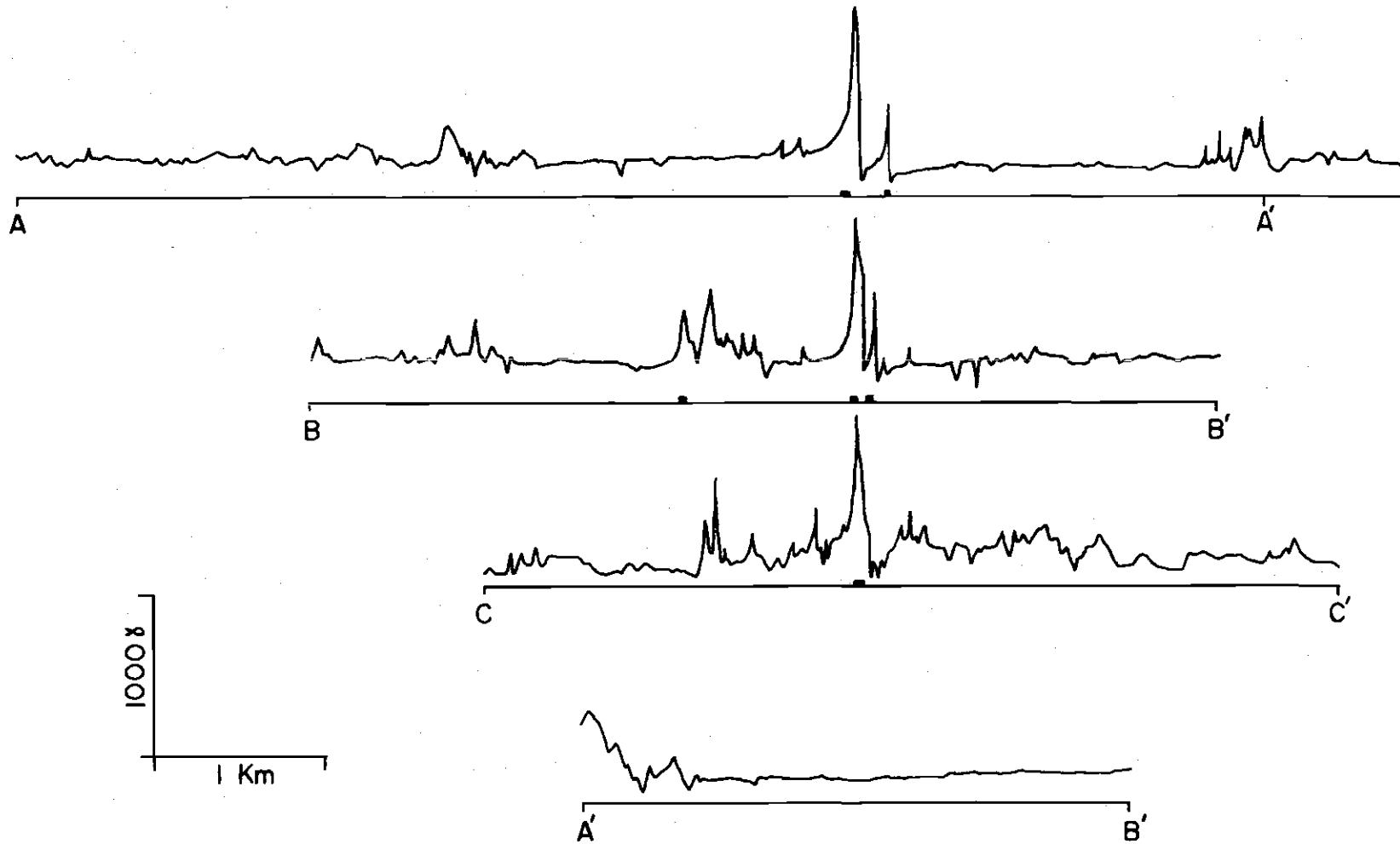


Figure 8. Ground-Level Magnetic Profiles (Total Field). (Heavy bar on profile base indicates diabase outcrop. See Figure 7 for location of profiles.)

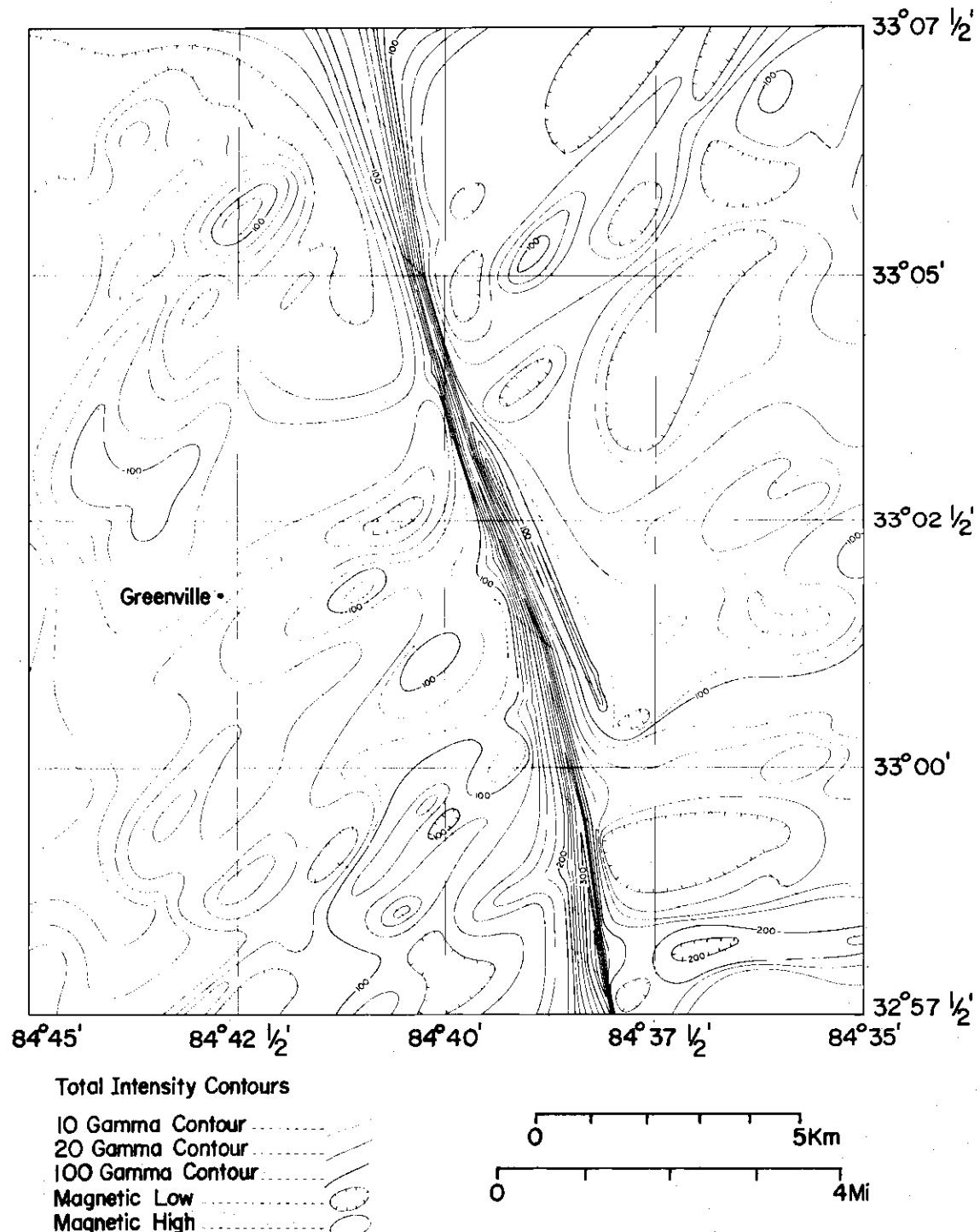


Figure 9. Aeromagnetic Map (Total Field) of the Study Area Recontoured Assuming the Meriwether Dike to be a Continuous Magnetic Feature. (Anomalies are with reference to 55,000 γ datum.)

CHAPTER III

PHYSICAL PROPERTIES OF THE MERIWETHER DIKE

Density

Diabase lends itself especially well to geophysical investigation. The density of the Meriwether diabase is $3.0 \pm 0.05 \text{ gm/cm}^3$ (as determined by gravimetric methods applied to three field samples). Watson (1902) determined the densities of the Loachapoka Schist and local granites to be $2.64 \pm 0.01 \text{ gm/cm}^3$ and $2.70 \pm 0.01 \text{ gm/cm}^3$ respectively. Thus, the density contrast between the diabase of the Meriwether dike and the surrounding rocks (average density $2.67 \pm 0.02 \text{ gm/cm}^3$) is $0.33 \pm 0.07 \text{ gm/cm}^3$. A vertical dike 30 meters wide (average observed outcrop width of the Meriwether dike) with this density contrast should yield a vertical gravity anomaly of approximately 1.5 milligals, an anomaly easily discerned with contemporary instrumentation (see Appendix I).

Magnetic Susceptibility

Several attempts have been made to statistically relate the bulk susceptibility of rocks to petrological parameters. One such attempt was that of Balsey and Buddington (1958) who related the susceptibility of some Adirondack rocks to the fractional volume of all the minerals visually identified as magnetite. This volume would generally include any Fe-Ti oxide minerals of spinel structure. Their empirical formula for the bulk susceptibility (k) in C.G.S. units is

$$k = 2.6 \times 10^{-3} V^{1.11} \quad (1)$$

where V is the volume percentage of all minerals visually identified as magnetite.

Petrographic examination of the Meriwether dike (Lee, 1971) showed that opaque grains (assumed to be Fe-Ti oxides of spinel structure) comprise 2.3 to 4.3 percent of the rock with a higher percentage occurring in the finer-grained zones near its edges. Using the empirical formula of Balsey and Buddington (1958) (Equation 1) and the range of volume percentages of opaques given by Lee (1971), the bulk susceptibility of the diabase composing the Meriwether dike was estimated to be between 0.0066 and 0.0130 cgs.

CHAPTER IV

DETERMINATION OF DIP ANGLE FROM GRAVITY
AND MAGNETIC ANOMALIESTheoretical Models

Theoretical anomalies were calculated for sets of models to examine the effects of dip angle on expected gravity and magnetic anomalies. The method of Talwani, Worzel, and Landisman (1959) was used to compute the gravity anomalies that would be expected for dikes dipping at various angles. Because the observed outcrop width would be fixed for a particular dike, anomalies were computed for models with an outcrop width of 30 meters dipping at 90, 75, 60, and 45° (Figure 10). As would be expected, the gravity anomaly caused by a vertical dike is symmetric about the center of the dike. However, as the dip angle decreases the anomaly becomes asymmetric with the peak shifting toward the direction in which the dike is dipping. The anomaly tails off more slowly on the side toward which the dike dips than the other. Even though there are obvious differences in the anomalies for various values of dip angles, a superimposed regional trend may make determination of the dip more difficult than suggested by Figure 10; in fact, unless the regional trend is simple and well defined, the determination of the dip may be impossible.

Although the dip angle has an obvious effect on the shape and asymmetry of the total-field anomaly (Figure 11), the effects of natural

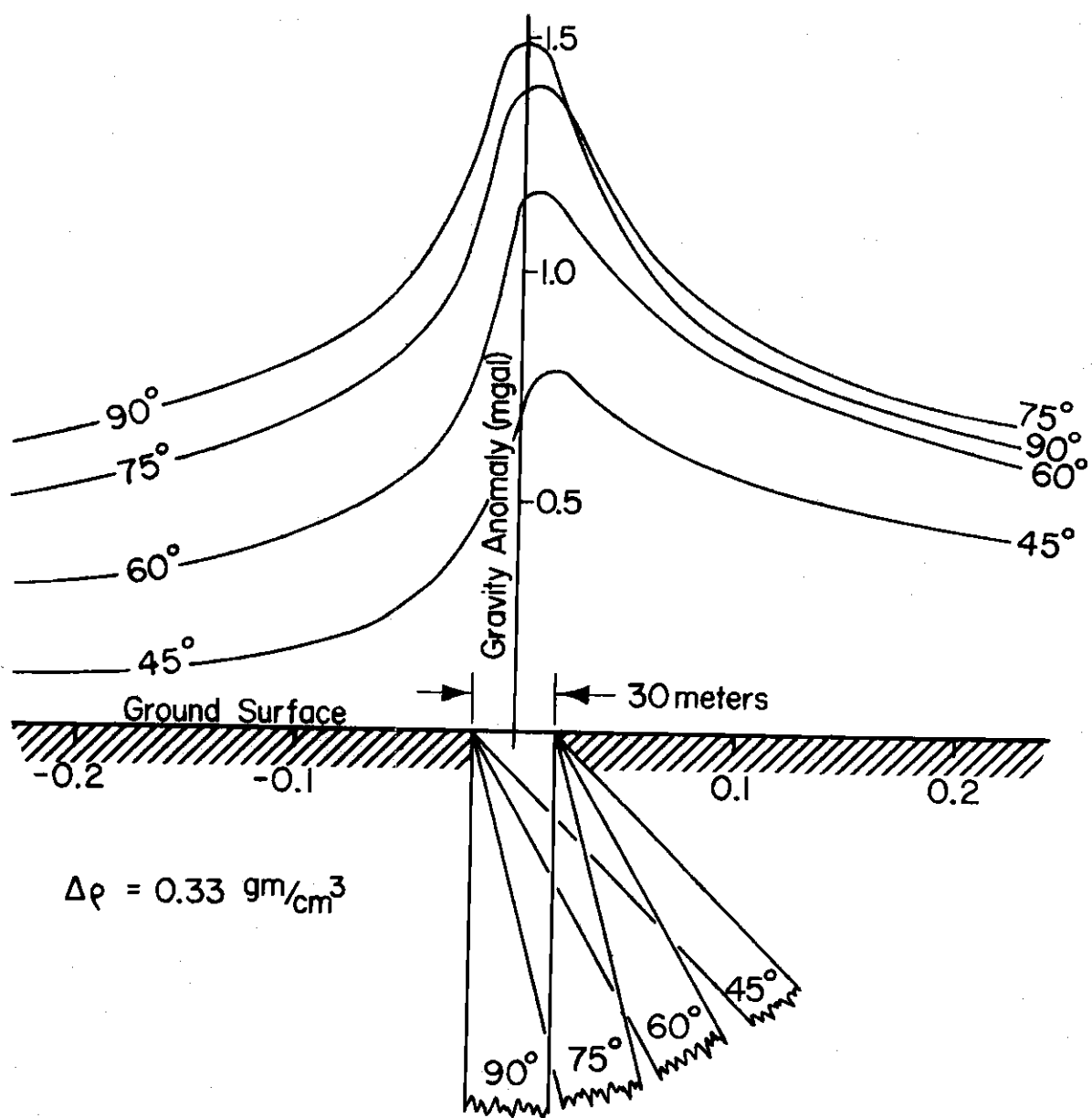


Figure 10. Calculated Curves Showing Effect of Dip Angle on Vertical Gravity Anomaly.

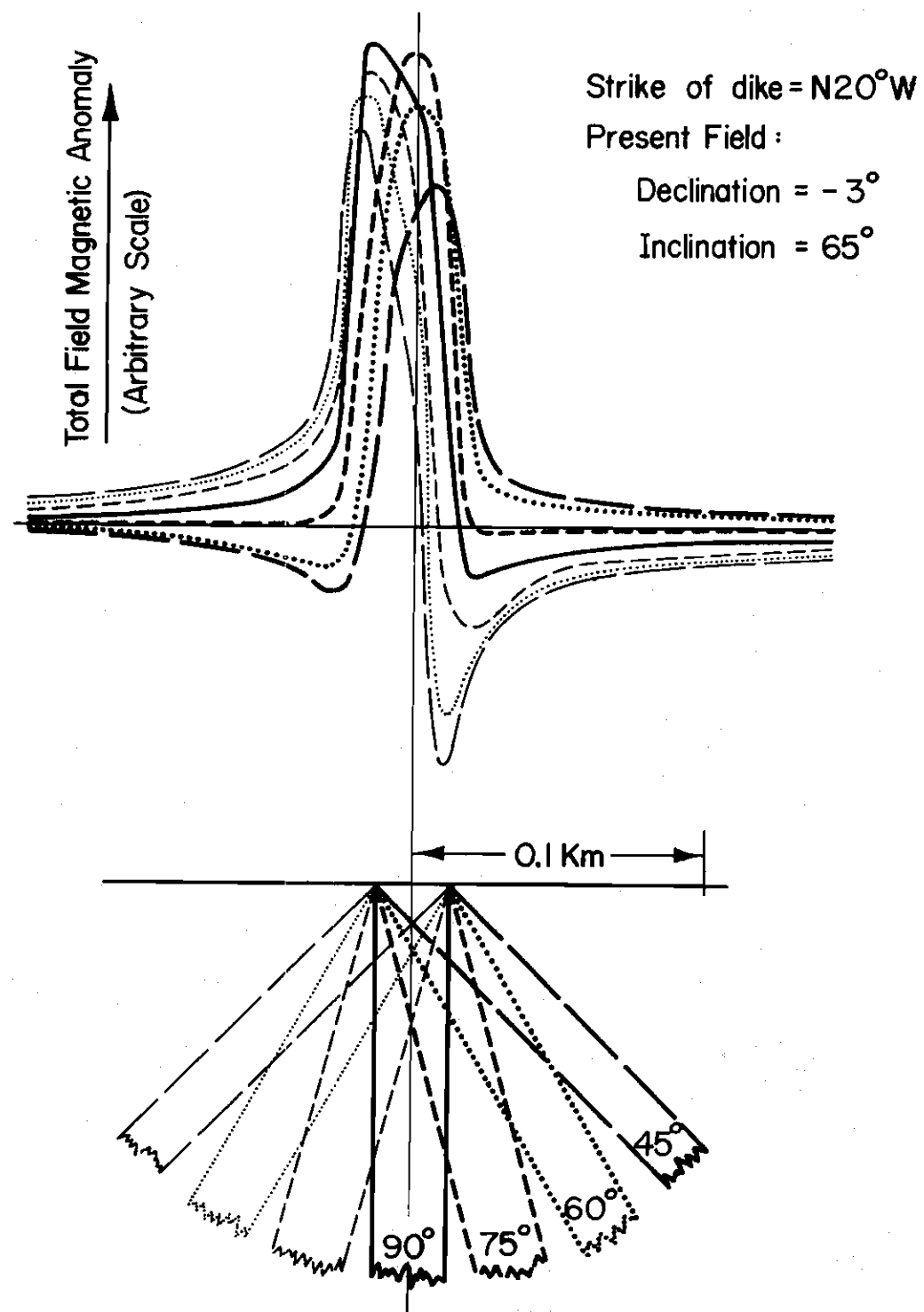


Figure 11. Calculated Curves Showing Effect of Dip Angle on Total Field Anomaly Due to Induction Magnetization Only.

remanent magnetization, when added to the induced magnetization, may complicate the determination of dip angle from the observed anomaly (Hood, 1963). For this reason, the angle of dip was determined using observed gravity anomalies only. The magnetic anomalies, because of their sharpness as compared to the gravity anomalies (Figures 8 and 10), were used only for lateral location of the dike where outcrops were nonexistent.

Detailed Gravity Profiles

Five detailed gravity lines with an average station spacing of 0.15 kilometers and a total length of 20 kilometers were obtained. Station spacing was decreased to about 0.075 kilometers in the immediate proximity of the dike. Four lines traverse the Meriwether dike in the prescribed study area (Figure 4) and the fifth traverses it along Georgia State Highway 16 southeast of Newnan and north of the study area. The observed anomalies (Figures 12 through 16), when smoothed, are about 1.0 kilometer wide at half their maximum value. This width is considerably greater than the computed anomaly width for a vertical dike 30 meters wide, approximately 0.1 kilometers at half its maximum value (Figure 10). Numerous individual peaks superimposed on the broad peaks suggest that a 0.75 kilometer wide swarm of dikes, rather than a single dike, is responsible for the observed anomaly. Such a hypothesis is further supported by the ground-level magnetic profiles, (Figure 8).

Profile A-A'.

Gravity line A-A' (Figure 4) was established along a dirt road about 3.0 kilometers north of Georgia State Highway 109. The observed

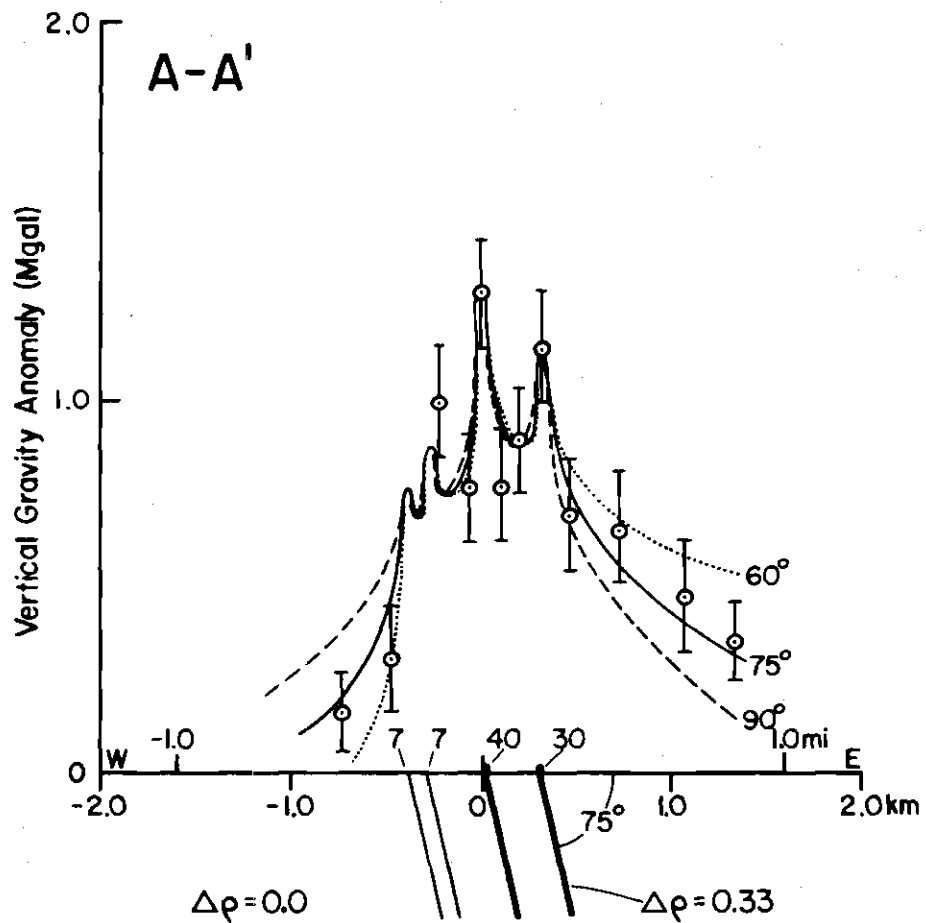


Figure 12. Detailed Gravity Profile A-A'. (Model dikes extend to infinite depth. Thickness of the modeled dike is given by the numeral above the dike. Heavy bar on profile indicates observed dike outcrop.)

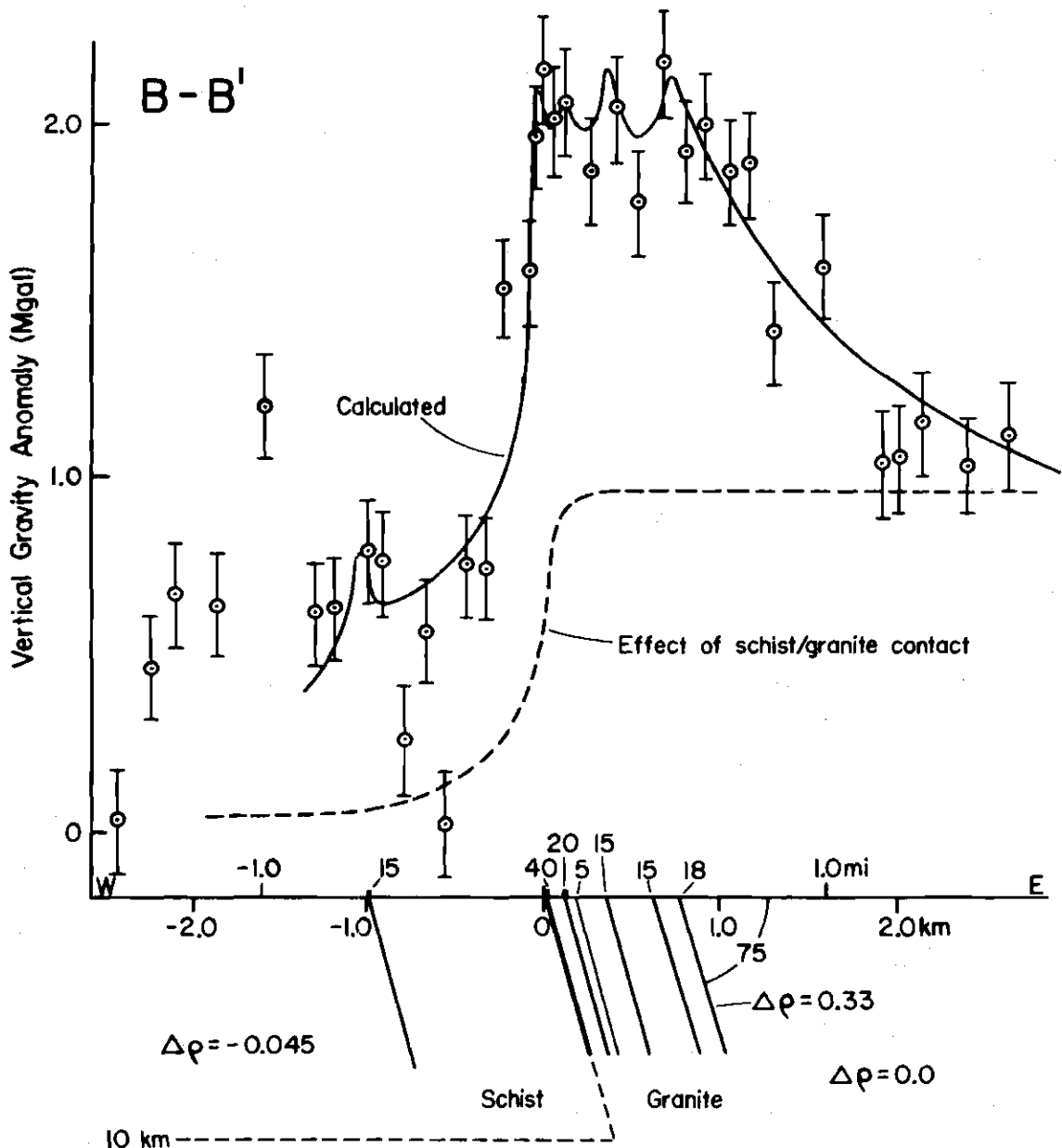


Figure 13. Detailed Gravity Profile B-B'. (Model dikes extend to infinite depth. Thickness of the modeled dike is given by the numeral above the dike. Heavy bar on profile indicates observed dike outcrop.)

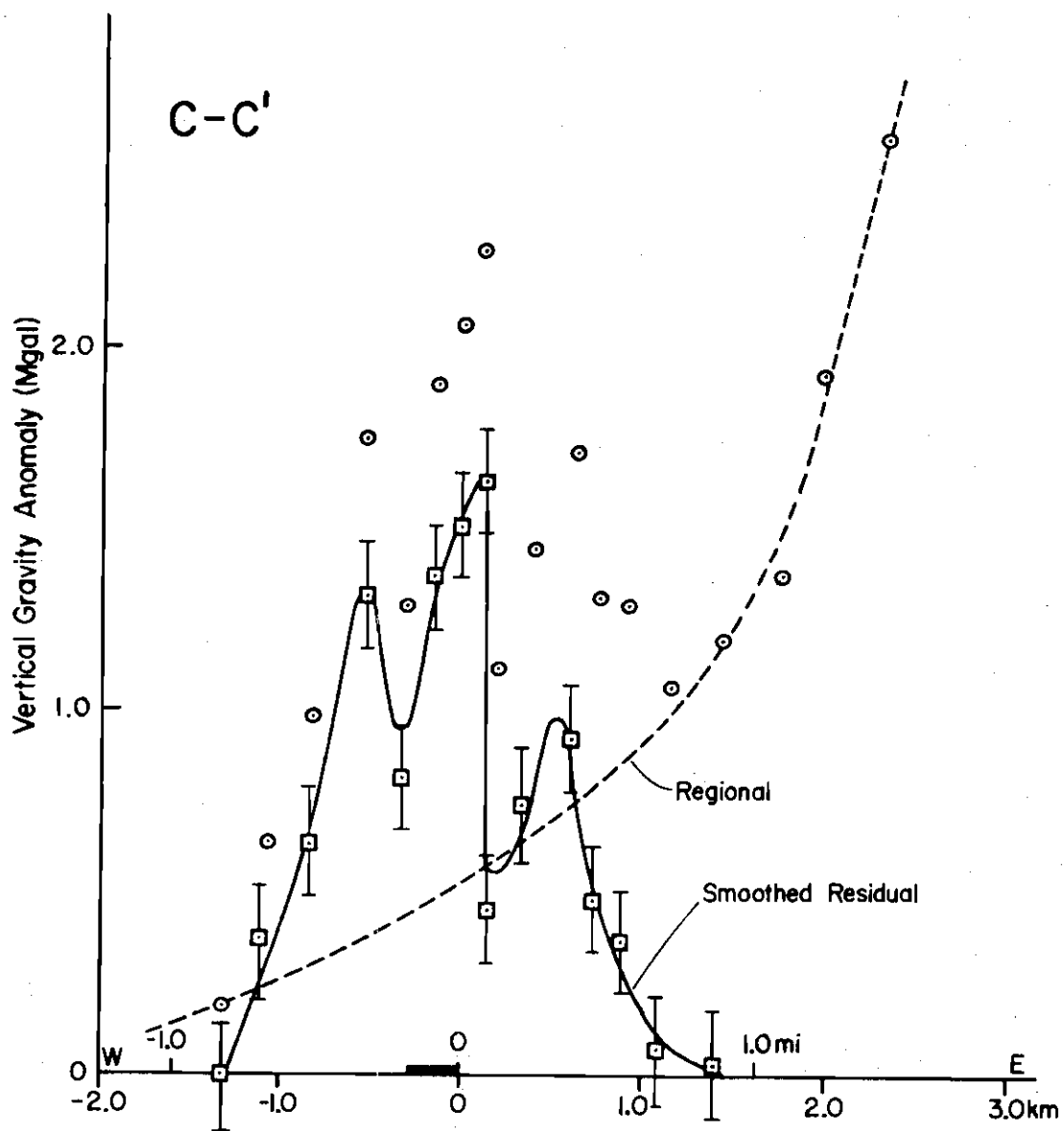


Figure 14. Detailed Gravity Profile C-C'. (Smoothed residual exhibits three definite peaks. Heavy bar on profile indicates observed dike outcrop.)

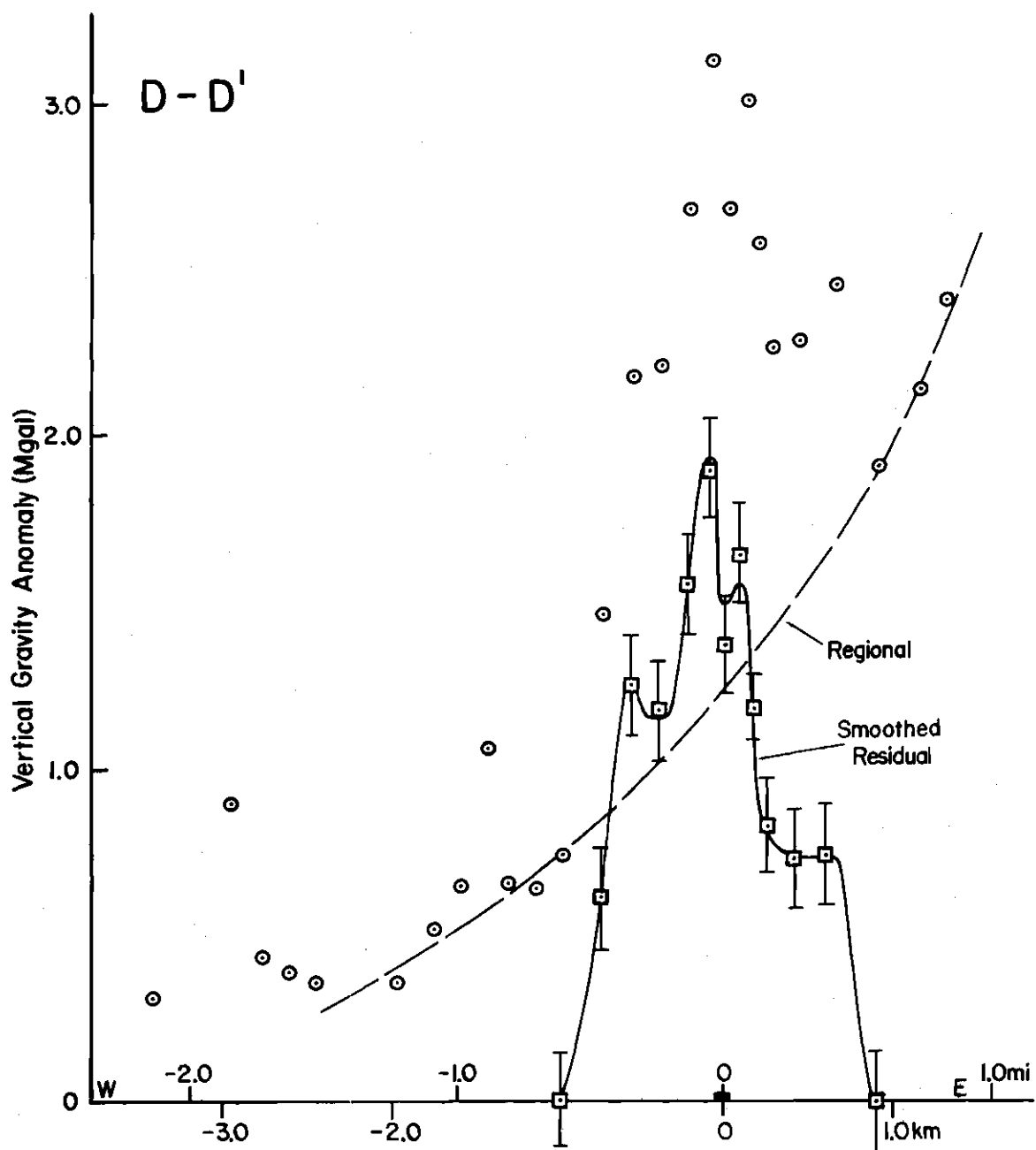


Figure 15. Detailed Gravity Profile D-D'. (Smoothed residual exhibits multiple peaks. Heavy bar on profile incidates observed dike outcrop.)

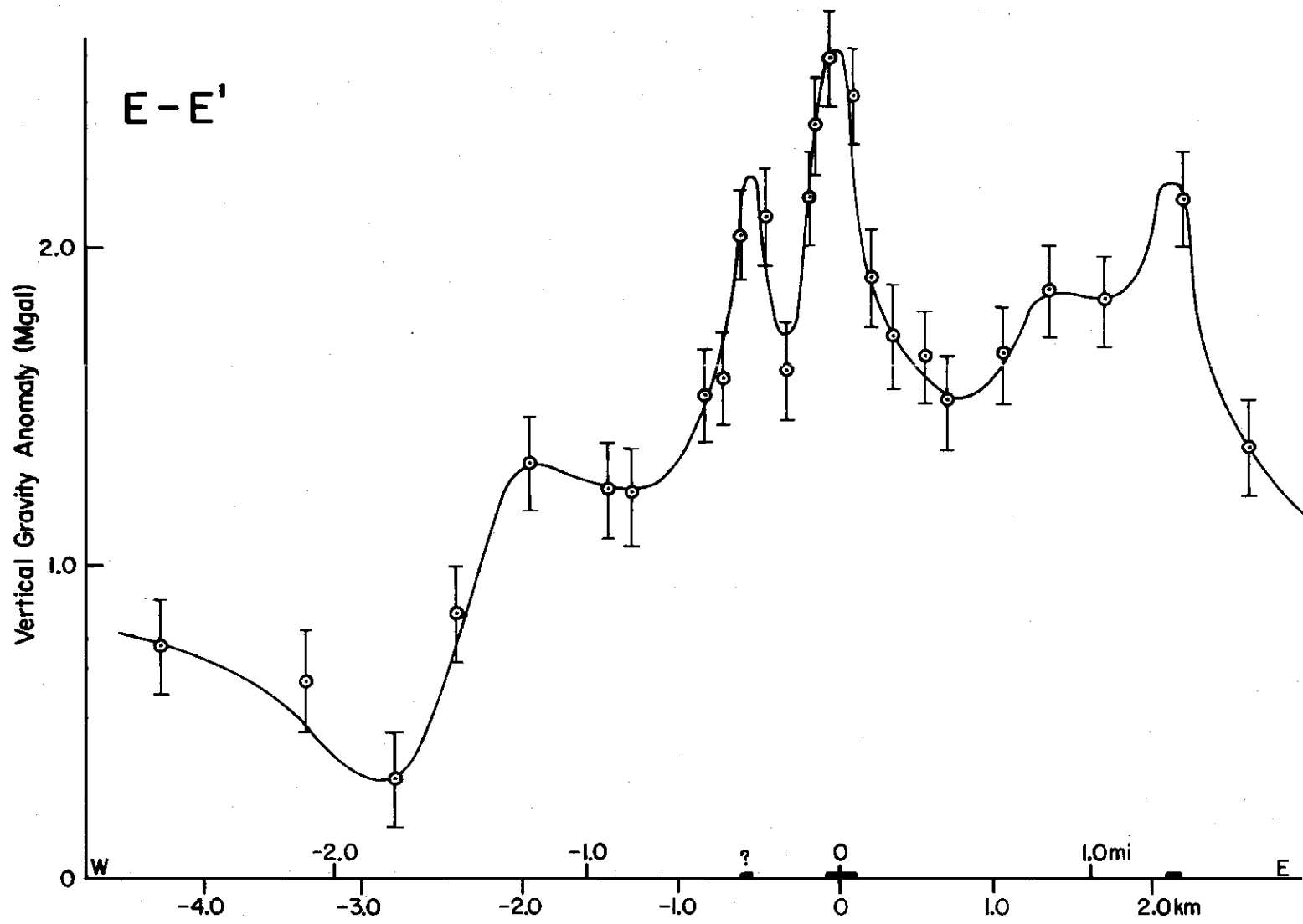


Figure 16. Detailed Gravity Profile E-E'. (Georgia Highway 16, south of Newnan. Heavy bar on profile indicates observed dike outcrops.)

gravity anomaly (Figure 12) consists of three peaks of about one milligal amplitude with the side and less prominent peaks spaced about 0.2 kilometers to either side of the main peak. Because there exist no known density anomalies, with exception of the diabase, along this profile and because the regional isogals are slightly curved in the region of this profile (Figure 4), no regional trend was removed. The three peaks and the asymmetry of the anomaly suggest that three dikes dipping to the east are necessary to account for the observed anomaly. Examination of the ground-level magnetic data for the same profile (Figure 8) suggests that the side dike to the west is actually two thin dikes. Assuming the existence of the four dikes, anomalies were computed using the observed outcrop widths for the main dike (40 meters) and the east dike (30 meters). The west dikes were not found to outcrop and because of the lesser magnitude of the associated gravity anomaly as compared to those of the main dike, they were modeled to be 7.5 meters wide.

Examination of the computed anomalies for dips of 90, 75 and 60° (Figure 12) shows the observed anomaly to fall between the computed curves for 60 and 75 with a dip angle of 70° (by interpolation) probably best satisfying the observed data.

Profile B-B'.

Detailed gravity line B-B' (Figure 4) was established along Georgia State Highway 109 between Greenville and Gay, Georgia. The observed anomaly consists of a "noisy" assymmetric broad peak (Figure 13). Amphibolites were found outcropping to the west of the main dike and could be responsible for the observed scatter in the data west of the dike. Diabase float was also found 1.0 kilometers west of the main

dike indicating that part of the observed scatter in the data may be a result of a side dike. A corresponding magnetic anomaly was encountered during the ground-level magnetic survey of the same profile (Figure 8).

Aside from the scatter in the data to the west of the main dike, there is a difference in the base level of the observed gravity. The east side of the dike is about 1.0 milligal more positive than the west side. This offset can be accounted for by the contact (no fault is visible and the orientation of the contact is unknown) between the Loachapoka Schist to the west and the granite to the east.

After the effect of the contact was removed, the resulting asymmetric residual anomaly could be modeled by a set of six dikes dipping to the east. Only the main dike was observed to outcrop, but the ground-level magnetic data (Figure 8) indicate the existence of the others. Determination of the angle of dip was not attempted because of the uncertainty in the location and orientation of the schist-granite contact.

Profile C-C'.

Profile C-C' (Figure 4) was established along the dirt road about 1.5 kilometers south of Georgia State Highway 109. The strong eastward positive trend of the observed data (Figure 14) is probably caused by granitic rocks which dip westward (Figure 3). Because the exact location and attitude of the granite-schist contact were unknown, a regional trend was estimated (Figure 14). The residual anomaly (Figure 14) consists of a central main peak and two secondary peaks on either side of the main peak. Although the dike was found to outcrop only coincident with the central peak of the gravity anomaly, the secondary peaks of the anomaly are probably due to side dikes. A similar phenomenon was

noted previously for profiles A-A' and B-B' further to the north. Because of the ambiguity created by the removal of the regional gravity trend by smoothing, and the noisy character of the ground-level magnetic data taken for the same profile (Figure 8), no attempt was made to determine the dip angle of the dikes.

Profile D-D'.

Line D-D' (Figure 4) was established along the paved county road about 8.0 kilometers southeast of Greenville and 4.5 kilometers south of detailed gravity line C-C'. As in profile C-C', there is a strong positive regional trend to the east (Figure 15), which was removed. The multiple peaks in the residual anomaly, (Figure 15) although not as well separated as in the previous profiles, again indicates that more than one dike is responsible for the observed anomaly. The only dike found to outcrop was again coincident with the main peak.

Profile E-E'.

Gravity line E-E' lies along Georgia Highway 16, southeast of Newnan. This profile, which is outside the main area of investigation, was obtained for comparison to the four previous profiles which lie within the area of detailed study 20 kilometers to the south. The observed anomaly (Figure 16) consists of three peaks all coincident with observed outcrops of dikes with the central peak corresponding to the widest outcrop. Whereas the side dikes in profiles to the south are located no more than 1.0 kilometers to the side of the main dike, the east dike on profile E-E' is located 2.1 kilometers from the main dike.

CHAPTER V

GROUND-LEVEL MAGNETICS AND THE ROLE OF NATURAL REMANENT
MAGNETIZATION IN THE OBSERVED ANOMALIESGround-Level Magnetics

Four detailed ground-level magnetic (total field) profiles were obtained in order to examine the structure of the Meriwether dike and to provide additional data for the purpose of recontouring the aeromagnetic data previously described. Three of the profiles were obtained along the same roads as detailed gravity profiles A-A', B-B', and C-C'. The fourth was a closure profile connecting A-A' and B-B' (Figure 7). The data was obtained and reduced by standard techniques and are listed in Appendix II.

The reduced data (Figure 8) showed the main dike to be represented by an asymmetric anomaly for all three profiles. However, the calculated anomaly due to induction magnetization for a dike dipping 70° toward N70°E is a symmetric positive peak (Figure 11). This suggests that induction magnetization is not the only cause for the observed anomaly and that natural remanent magnetization (NRM) must also be considered in the analysis of magnetic anomalies (Hood, 1963).

Natural Remanent Magnetization of the Meriwether Dike

Samples from a single outcrop of the Meriwether dike were collected and analyzed for NRM by Doyle Watts (personal communications). Intensities and directions for the NRM's are given in Appendix IV. A

Schmidt stereographic projection of the NRM directions (Figure 17) shows the NRM directions to be different from today's magnetic field. Samples from the center of the dike constitute one set of directions and those from the chilled margins another set. Because it is not known what proportion of the dike has which magnetization, an average of the directions (Figure 17) and magnitudes were used for computing the anomaly due to remanent magnetization. The average direction has a declination of 28° and an inclination of 30° . The average magnitude of the NRM is 0.00175 cgs.

Theoretical Anomalies and the Determination
of the Koenigsberger Ratio, Q

The ratio of remanent magnetization to induced magnetization, the Koenigsberger ratio, Q is commonly cited in paleomagnetic studies as an indication of whether or not samples have been subjected to lightning strikes. It has more recently been construed (Green, 1960) as a measure of the importance of remanent magnetization in the analysis of magnetic anomalies. Using the calculated bulk susceptibility for the diabase of the Meriwether dike and the average intensity of NRM, the probable range of Q is 0.25 to 0.50. The range of Q's is a result of the uncertainty in the bulk susceptibility.

To examine the effects of Q on the observed anomalies, several models were computed using the method of Talwani and Heirtzler (1965). For a Q of 0.25 and bulk susceptibility of 0.013 cgs, the remanent magnetization causes the anomaly to become slightly asymmetric (Figure 18) with a peak to trough ratio of about 15 to 1. For bulk suscepti-

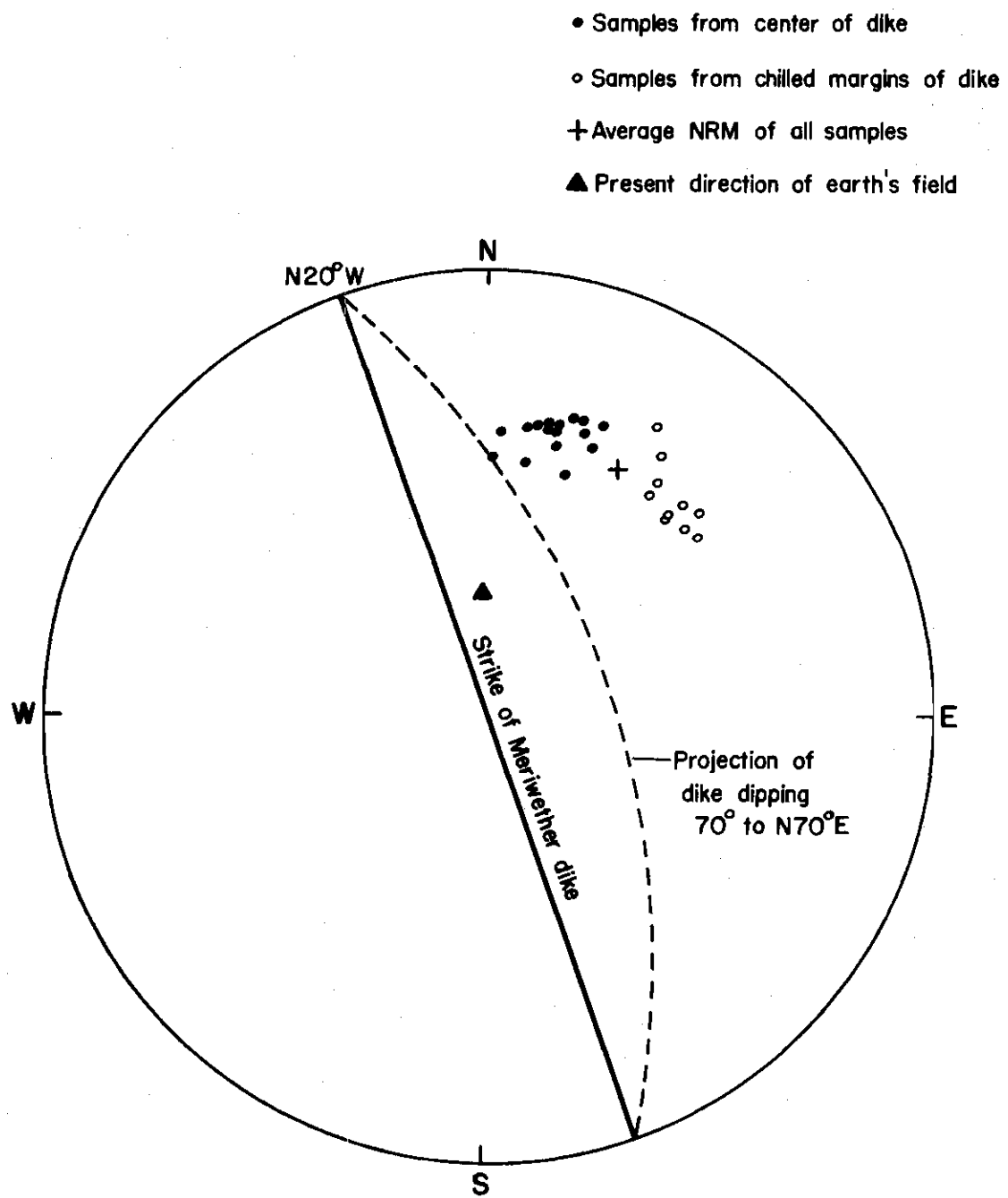


Figure 17. Stereographic Projection (Schmidt net) of Measured Natural Remanent Moments (NRM) for the Meriwether Dike.

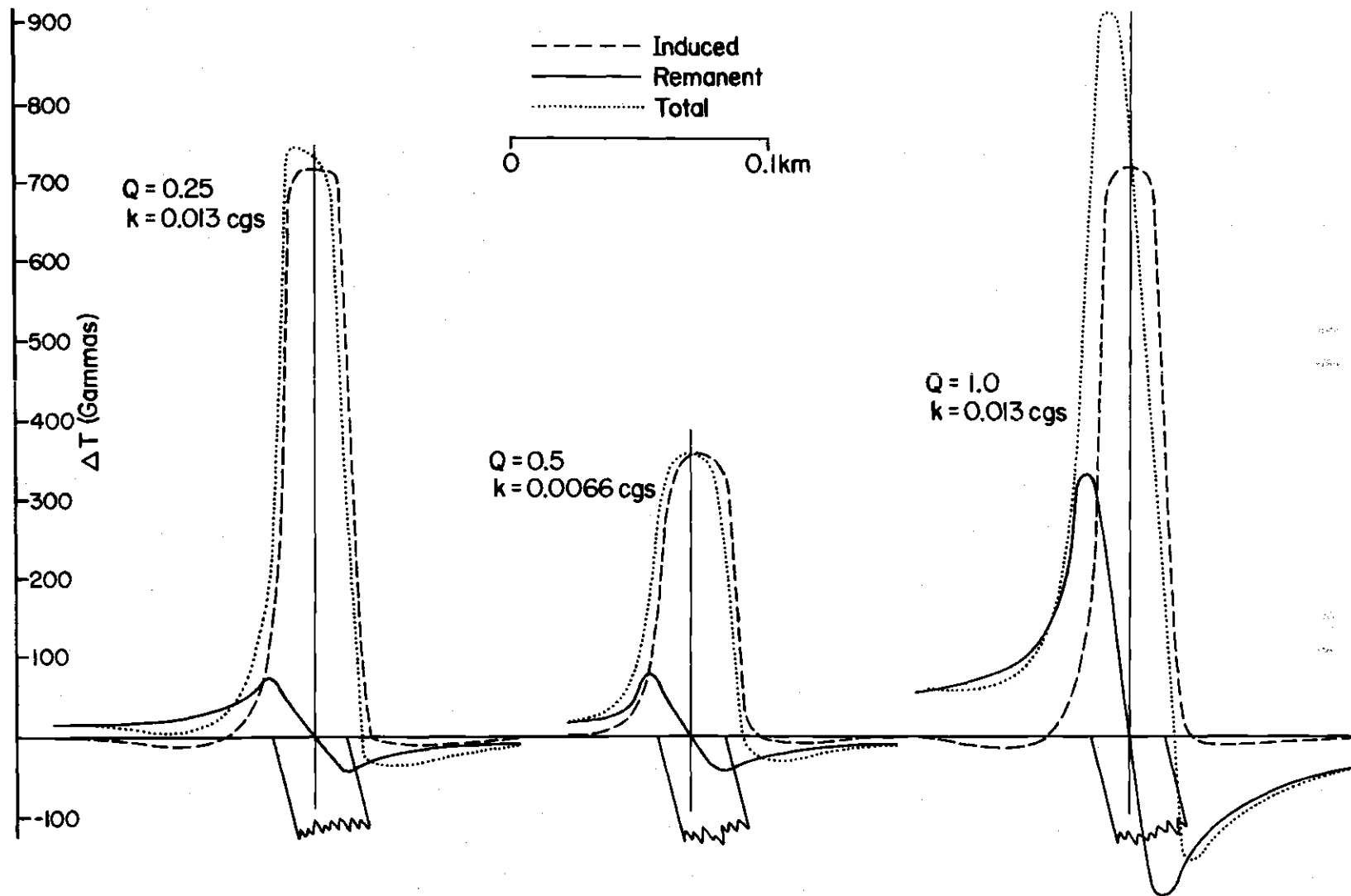


Figure 18. Calculated Curves Showing the Effect of Natural Remanent Magnetism on the Total Field Anomaly. (Dike is 30 meters wide and dips at 75° .)

bility 0.0066 cgs and corresponding Q of 0.5 the anomaly is found to be more asymmetric with a peak to trough ratio of 10 to 1.

The observed anomalies (Figure 8) however, exhibit an average peak to trough ratio of only 6. Further, the amplitude of the observed anomalies is greater than that calculated for the given range of susceptibilities and corresponding magnetizations. An increase in Q to 1.0 at a susceptibility of 0.013 cgs produced an asymmetric anomaly with a peak to trough ratio of about 6 to 1, (Figure 18) indicating that the bulk remanent magnetization was probably greater than that suggested by the surface samples.

Strangway (1965), who sampled a diabase dike at both the surface and at depth in a mine, found the ratio of remanent to induced magnetization to be greater for the underground samples. As a possible cause of this phenomenon Strangway (1965) suggests that temperature fluctuation at the surface, which was probably exposed for a considerable length of time, has accelerated the decay of the remanent magnetization. The same type of process may have occurred in the Meriwether dike and hence, the effective Q, which includes the effect of sub-surface portions of the dike, is probably closer to 1.0.

It should be noted that even if the dike actually dips as much as 80° , the magnetic anomaly due to induction would still be a symmetric peak (Figure 11), and hence the calculated Q of 1.0 would not be seriously affected.

CHAPTER VI

DISCUSSION AND CONCLUSIONS

Examination of the Meriwether dike by means of detailed gravity and magnetic profiles shows the dike to consist of an injection zone of dikes. Because the gravity anomalies of the component dikes are only partially separated, determination of whether or not the side dikes were branches of the main dike was not possible. On the basis of theoretical curves for the dike system dipping at various angles, the Meriwether dike (system) was estimated to dip at 70° toward N 70° E.

The 70° dip is not as steep as noted by Lester and Allen (1950), who found several of the larger dikes in Georgia to have a constant dip toward the east of 75 to 90° and Privett (1966) who found the diabase dikes in central South Carolina to dip 80 to 90° to the NE. It is possible, however, that the Meriwether dike may actually have a dip greater than 70° , but due to the ambiguity of the regional trend it is not possible to resolve how much greater.

A simple Bouguer gravity map compiled for central Meriwether County shows the Meriwether dike to be responsible for an anomaly of one to two milligals in the regional trend. After recontouring of the available aeromagnetic data, the Meriwether dike(s) proved to be the most prominent magnetic feature of the area, and this suggests that the sharpness of the anomaly and the flight line spacing suppressed the dike(s) in previous contouring. It is possible that in other areas of

eastern North America covered by aeromagnetic maps, other occurrences of diabase dikes may be similarly suppressed, thus reducing the probability of locating such dikes by their magnetic anomalies in areas not yet geologically mapped. Locating other dikes by this method may also be hampered by the effects of remanent magnetization.

Although not studied in detail, examination of high altitude infrared photographs (N.A.S.A., 1970) of central Meriwether County, revealed the existence of a linear anomaly coinciding with the Meriwether dike at known outcroppings in the northern third of the study area. The anomaly is probably due to a change of intensity of reflected infrared radiation from the vegetation growing in the soil derived from the diabase. It is suggested that this technique might be applied to other areas of eastern North America to determine outcrop patterns of the dikes in areas not yet geologically mapped.

Many problems currently exist concerning the diabase dikes which surround the North Atlantic Ocean such as dating, distribution and chemistry. It is hoped that more economic and efficient methods such as those suggested in this study will lead to the location of unmapped dikes, thus presenting a more complete picture of the distribution and role of these dikes in the history of the opening of the North Atlantic Ocean.

APPENDICES

APPENDIX I

GRAVITY SURVEYS AND DATA REDUCTION

Gravity data were collected and reduced by standard techniques (Dobrin, 1960). The data consist of 242 points in total including base stations - 201 gravity observations are along five detailed lines and 41 gravity observations are regional data.

The gravimeter used was the Worden Educator, Model 113. The reading precision of this meter, when read by a single operator, is approximately ± 0.1 milligals. Instrumental drift for the Worden gravimeter for an eight hour period is typically 0.2 milligals, but can be as high as 0.5 milligals for the same period. The gravimeter was stored in the field vehicle each night preceding a survey to minimize the instrumental drift due to temperature change. The uncertainty in drift and reading precision combined give a gravity precision of ± 0.2 milligals. In all, three different base stations (Dorman and Ziegler, in preparation, Georgia Department of Mines, Mining and Geology) were used to correct for instrumental drift. Pertinent data concerning these base stations are given in Table 1.

The observed drifts are given in Table 2.

Table 1. Gravity Base Stations Used in this Study

<u>Name</u>	<u>Base Number</u>	<u>Location</u>	<u>Gravity Value</u>	<u>Estimated Precision</u>
Atlanta D	4	Georgia Tech	979527.37	<u>+0.023</u>
LaGrange	33	City Hall	979484.42	<u>+0.014</u>
Greenville	63	Meriwether County Court House	979489.58	<u>+0.05</u>

Table 2. Instrumental Drift for Worden Gravimeter

<u>Station Nos.</u>	<u>Georgia Tech Gravity Survey No.</u>	<u>Drift (Mgals/hr)</u>	<u>Time Between Base Stations</u>
1 - 49	36	-0.074	6.1 hours
1 - 33	46	-0.018	9.8
1 - 48	51	0.000	7.4
48 - 72	51	-0.109	3.9
72 - 95	51	0.016	2.3
4 - 20	52	-0.053	2.8
20 - 41	52	-0.121	3.8

The gravity data were corrected for latitude effect by using the international gravity formula of 1930 (as given in Dobrin, 1960, page 187) and drift corrections for the meter by assuming linear meter drift between subsequent occupations of the base station. The standard Bouguer reduction density of 2.67 gm/cm^3 was used to compute the Bouguer anomalies.

Elevation and location control were obtained from the following U. S. Geological Survey, $7\frac{1}{2}$ minute topographic maps: Greenville (1971), Gay (1971), Warm Springs (1971), and Woodbury (1971). Where possible bench marks (± 1 foot) or intersection elevations (assumed ± 5 feet) were used. Elevations of stations for which bench marks or intersections were not available were obtained by interpolating between contour lines (20 foot contour interval) and confirming those interpolations with barometric altimetry data. Elevations obtained by this technique were estimated to be plus or minus five feet. The resulting uncertainty in the reduced gravity values is thus ± 0.35 milligals. Because of the relatively shorter distance between stations along detail lines, and hence shorter times between gravity and barometric readings errors in drift for these measurements were considered less. This results in an estimated precision of ± 0.2 milligals for the reduced gravity values for stations along detail lines.

The data, in the standard Department of Defense computer card format, are listed by individual surveys in Table 3 (Figure 19).

ACIC HQ FORM NOV 68 0-154

PREVIOUS EDITION OF THIS FORM WILL BE USED UNTIL STOCK IS EXHAUSTED

DoD GR

Figure 19. Standard Department of Defense Gravity Coding Form.

Table 3. Gravity Data

Gravity Survey GT 36 (Includes Data for Profile B-B')

Table 3. (Continued)

Gravity Survey GT 46 (Includes Data for Profile E-E')

Table 3. (Continued)

Gravity Survey GT 51 (Includes Data for Profiles A-A', C-C', and D-D')

Table 3. (Continued)

Gravity Survey GT 51 (Continued)

Table 3. (Concluded)

Gravity Survey GT 52 (Regional Data)

APPENDIX II

GROUND LEVEL MAGNETIC SURVEYS AND DATA REDUCTION

Measurements of the magnitude of the geomagnetic field were made using a Geometrics Model G-816 proton-precession magnetometer. The digital display has a resolution of ± 1 gamma. The sensing element of the magnetometer is held at the end of an eight foot aluminum staff to suppress the magnetic effects of iron debris, e.g., beverage cans, small underground pipes, etc.

The data were reduced using standard techniques (Dobrin, 1960). The data consist of three detailed lines along graded dirt roads and a fourth along a two lane asphalt highway (Georgia State Highway 109). Approximately 0.016 kilometer was paced off between stations. Division of the actual length of the profile line by the number of station intervals yielded the actual station spacing. Times, needed for drift corrections, were recorded every ten minutes and the stations between time readings were assigned a time by assuming a linear sampling rate.

The variation in the main field over the area of investigation has been removed by approximating a gradient of $8.45\gamma/\text{mile}$ at $N3^\circ W$ (Garland, 1971, Figure 17.2) by a simple latitude correction of $9.56\gamma/\text{minute}$. Corrections for the diurnal variation were made using magnetograms of the Geomagnetic Observatory in Fredericksburg, Virginia (Figures 20 and 21) which were obtained from the World Data Center A of the National Oceanographic and Atmospheric Administration in

Boulder, Colorado.

These records were digitized and the vertical and horizontal components were added vectorily to give the magnitude of the total field. The difference between the computed total field and the value for the base line was taken to be the diurnal variation in the total field at Fredericksburg. Since the diurnal drift at any one place on the earth has been shown to be directly related to the hour angle of the sun (Matshusita and Campbell, 1965, Chapter 3) a shift of twenty-eight minutes was made in the drift curve so that it could be applied to the area of investigation. The variation of the diurnal drift with respect to latitude is negligible for the difference between Fredericksburg, Virginia and Greenville, Georgia (see Matshusita and Campbell, 1965, Figure 8, pages 321-323).

The computed latitude and longitude, time (Eastern Daylight Savings), raw magnetic value and corrected total magnetic field for each station occupied are given in Table 4.

NOAA
FREDERICKSBURG, VA.
MAY 5 1973

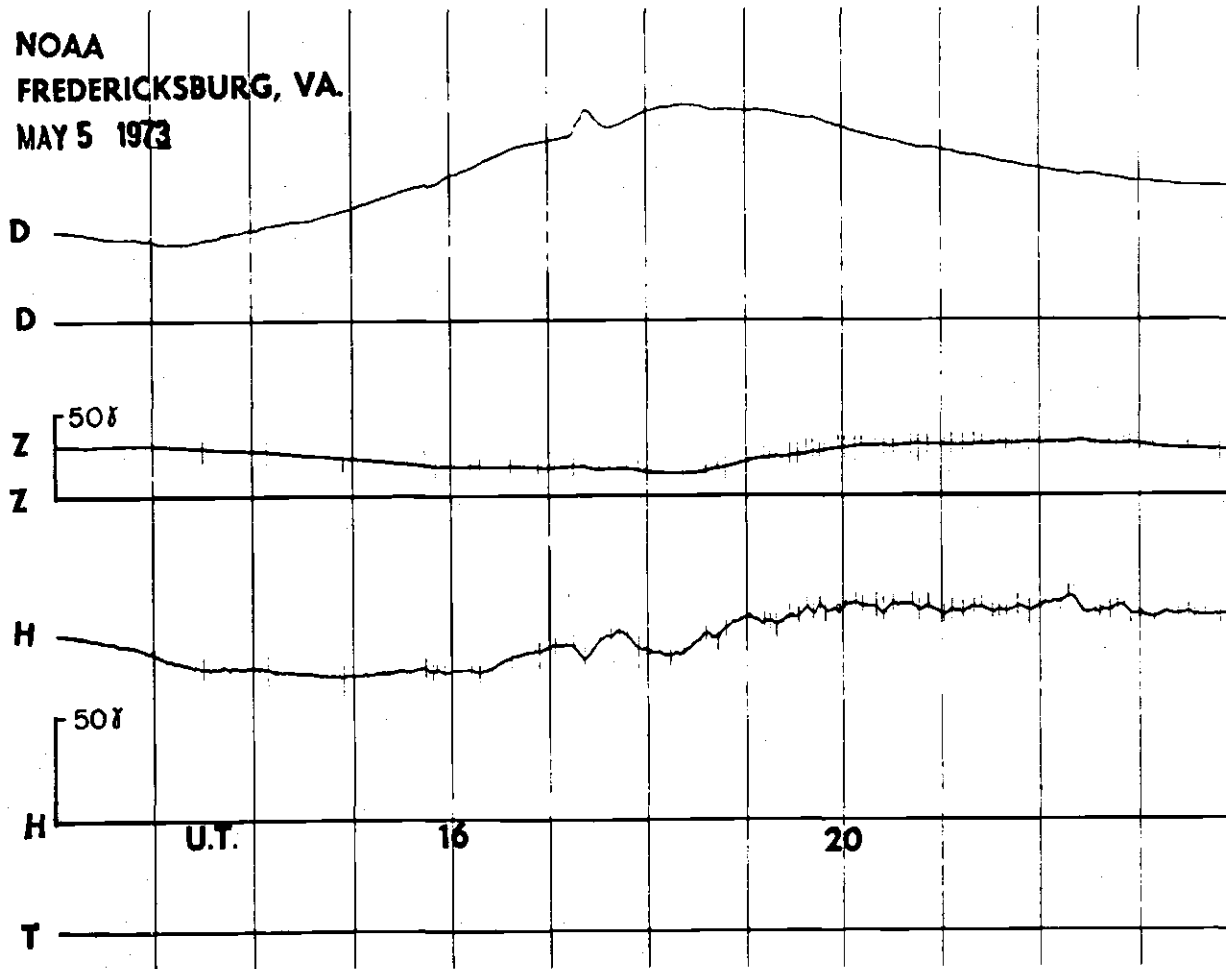


Figure 20. Magnetogram for May 5, 1973. (Courtesy National Oceanographic and Atmospheric Administration.

NOAA
FREDERICKSBURG, VA.
MAY 6 1973

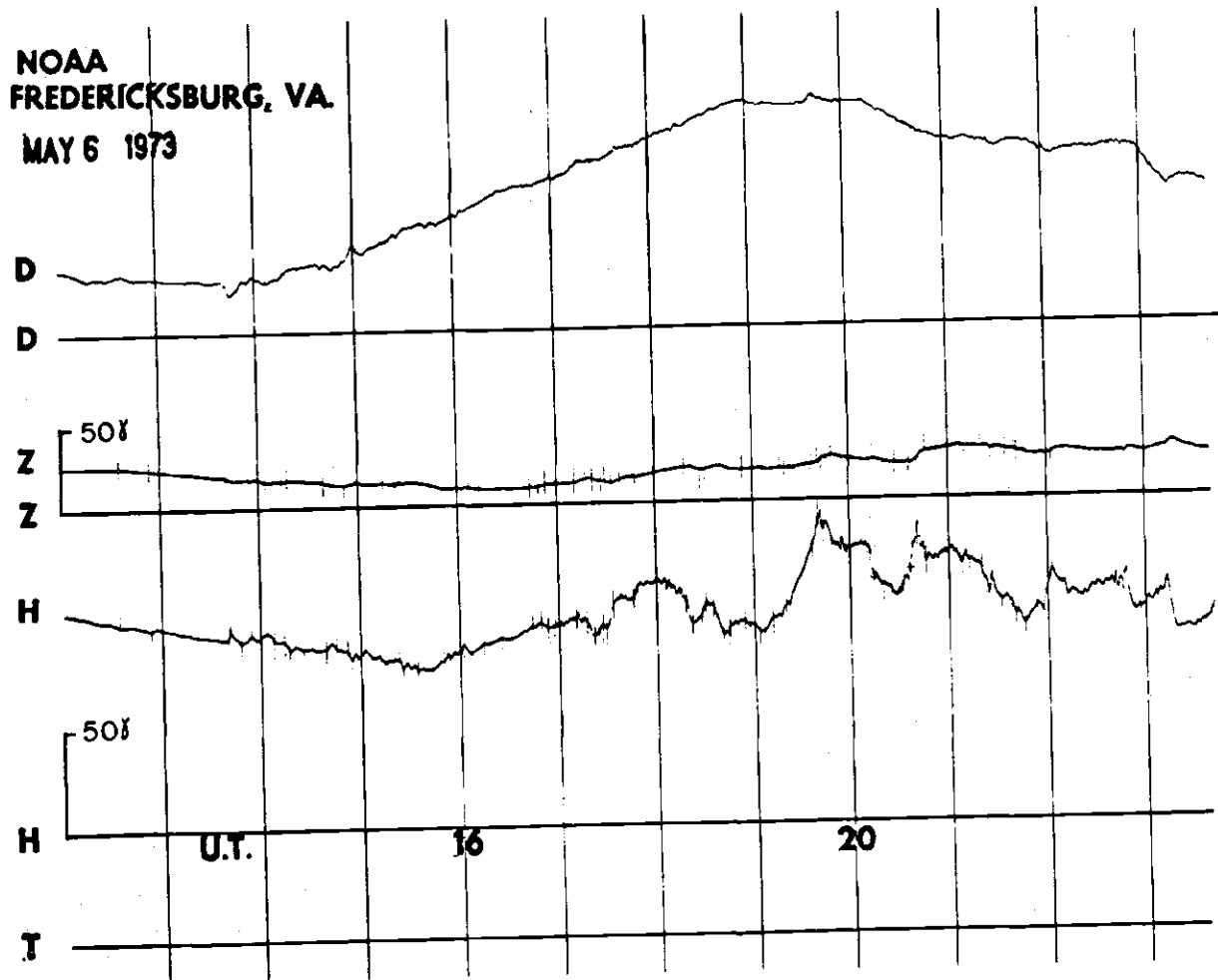


Figure 21. Magnetogram for May 6, 1973. (Courtesy National Oceanographic and Atmospheric Administration.

Table 4. Ground-Level Magnetics

Profile A-A', May 5, 1973

LATITUDE	LONGITUDE	TIME	RAW	REDUCED	LATITUDE	LONGITUDE	TIME	RAW	REDUCED
1234567890123456789012345678901234567890	1234567890123456789012345678901234567890				1234567890123456789012345678901234567890	1234567890123456789012345678901234567890			
33 3.030	84 42.670	15.483	53594	53631	33 3.477	84 41.493	16.345	53605	53644
33 3.078	84 42.673	15.495	53586	53622	33 3.488	84 41.481	16.357	53605	53645
33 3.126	84 42.676	15.507	53584	53620	33 3.500	84 41.468	16.368	53617	53657
33 3.174	84 42.680	15.518	5359n	53625	33 3.511	84 41.456	16.380	53593	53633
33 3.222	84 42.683	15.530	5359a	53633	33 3.523	84 41.444	16.392	53533	53573
33 3.270	84 42.686	15.542	5358a	53623	33 3.534	84 41.432	16.403	53617	53657
33 3.318	84 42.689	15.553	53609	53643	33 3.546	84 41.420	16.415	53622	53662
33 3.366	84 42.693	15.565	53603	53637	33 3.558	84 41.408	16.427	53625	53665
33 3.414	84 42.696	15.577	5361a	53651	33 3.569	84 41.395	16.438	53627	53667
33 3.461	84 42.699	15.588	53625	53658	33 3.581	84 41.383	16.450	53609	53649
33 3.509	84 42.702	15.600	53632	53665	33 3.592	84 41.371	16.462	53622	53662
33 3.557	84 42.706	15.613	5363n	53662	33 3.604	84 41.359	16.473	53702	53743
33 3.605	84 42.709	15.627	53636	53668	33 3.610	84 41.353	16.479	53721	53762
33 3.653	84 42.712	15.640	53640	53671	33 3.615	84 41.347	16.485	53709	53750
33 3.701	84 42.715	15.653	53586	53617	33 3.621	84 41.340	16.491	53705	53746
33 3.749	84 42.719	15.667	53616	53647	33 3.627	84 41.334	16.497	53699	53740
33 3.797	84 42.722	15.680	53617	53647	33 3.638	84 41.322	16.508	53667	53708
33 3.845	84 42.725	15.693	53571	53601	33 3.650	84 41.310	16.520	53581	53622
33 3.801	84 42.706	15.707	53594	53624	33 3.657	84 41.310	16.526	53647	53687
33 3.757	84 42.686	15.720	53569	53599	33 3.665	84 41.310	16.532	53629	53669
33 3.713	84 42.667	15.733	53595	53626	33 3.680	84 41.309	16.543	53616	53656
33 3.669	84 42.647	15.747	53604	53635	33 3.694	84 41.309	16.555	53601	53641
33 3.625	84 42.628	15.761	53606	53637	33 3.709	84 41.308	16.567	53589	53629
33 3.603	84 42.618	15.768	53607	53639	33 3.724	84 41.308	16.576	53583	53623
33 3.581	84 42.608	15.775	53802	53834	33 3.739	84 41.307	16.586	53587	53627
33 3.559	84 42.598	15.782	53604	53636	33 3.753	84 41.307	16.595	53579	53619
33 3.537	84 42.589	15.789	53612	53644	33 3.768	84 41.306	16.605	53584	53623
33 3.493	84 42.569	15.803	53613	53645	33 3.783	84 41.306	16.614	53602	53641
33 3.449	84 42.550	15.817	53635	53668	33 3.798	84 41.305	16.624	53593	53632
33 3.405	84 42.530	15.833	5361n	53645	33 3.812	84 41.305	16.633	53620	53659
33 3.407	84 42.500	15.850	5361a	53651	33 3.827	84 41.305	16.647	53656	53695
33 3.409	84 42.470	15.867	53617	53650	33 3.835	84 41.304	16.653	53741	53779
33 3.410	84 42.440	15.883	53617	53650	33 3.842	84 41.304	16.660	53821	53A59
33 3.412	84 42.409	15.900	53615	53648	33 3.849	84 41.304	16.667	53825	53A63
33 3.414	84 42.379	15.917	53624	53658	33 3.857	84 41.304	16.673	53840	53878
33 3.416	84 42.349	15.926	53605	53639	33 3.864	84 41.303	16.680	53786	53A24
33 3.417	84 42.319	15.935	5360a	53643	33 3.872	84 41.303	16.687	53760	53798
33 3.419	84 42.289	15.944	5360n	53635	33 3.879	84 41.303	16.693	5371n	53748
33 3.421	84 42.259	15.953	53605	53640	33 3.886	84 41.303	16.700	53633	53671
33 3.423	84 42.229	15.962	53590	53626	33 3.894	84 41.303	16.707	53679	53717
33 3.424	84 42.198	15.971	5360a	53644	33 3.901	84 41.302	16.714	53594	53632
33 3.426	84 42.168	15.979	53600	53636	33 3.909	84 41.302	16.722	53644	53681
33 3.428	84 42.138	15.988	53593	53629	33 3.916	84 41.302	16.729	53640	53677
33 3.430	84 42.108	15.997	53615	53652	33 3.923	84 41.302	16.736	53574	53611
33 3.431	84 42.078	16.006	53607	53644	33 3.931	84 41.301	16.743	53495	53632
33 3.433	84 42.048	16.015	53607	53644	33 3.938	84 41.301	16.750	53588	53625
33 3.435	84 42.018	16.024	53607	53644	33 3.945	84 41.301	16.758	53635	53672
33 3.437	84 41.987	16.033	53626	53663	33 3.953	84 41.301	16.765	53682	53719
33 3.439	84 41.957	16.053	53636	53674	33 3.960	84 41.300	16.772	53604	53641
33 3.440	84 41.927	16.072	5366n	53698	33 3.968	84 41.300	16.779	53603	53640
33 3.441	84 41.912	16.082	53655	53693	33 3.975	84 41.300	16.786	53620	53656
33 3.443	84 41.882	16.101	53655	53694	33 3.982	84 41.294	16.794	53581	53617
33 3.445	84 41.852	16.121	53644	53682	33 3.988	84 41.289	16.801	53587	53623
33 3.446	84 41.837	16.131	53635	53673	33 4.002	84 41.277	16.815	53593	53629
33 3.447	84 41.806	16.150	53629	53667	33 4.015	84 41.266	16.830	53574	53610
33 3.449	84 41.776	16.161	53639	53677	33 4.029	84 41.255	16.844	53633	53668
33 3.451	84 41.746	16.172	53619	53658	33 4.042	84 41.243	16.858	53625	53660
33 3.453	84 41.716	16.183	53694	53733	33 4.055	84 41.232	16.873	53666	53701
33 3.454	84 41.686	16.194	53617	53656	33 4.069	84 41.220	16.887	53637	53672
33 3.456	84 41.656	16.206	53607	53646	33 4.082	84 41.209	16.902	53601	53636
33 3.458	84 41.626	16.217	53603	53642	33 4.096	84 41.198	16.916	53564	53599
33 3.460	84 41.595	16.246	53616	53655	33 4.109	84 41.186	16.930	53565	53601
33 3.461	84 41.565	16.275	53601	53640	33 4.122	84 41.175	16.945	53567	53603
33 3.463	84 41.535	16.304	53587	53626	33 4.136	84 41.164	16.959	53576	53612
33 3.465	84 41.505	16.333	53604	53643	33 4.149	84 41.152	16.973	53343	53379

1234567890123456789012345678901234567890

Table 4. (Continued)

Profile A-A' (Continued)

LATITUDE	LONGITUDE	TIME	RAW	REDUCED
1234567890123456789012345678901234567890				
33 4.163	84 41.141	16.988	53597	53633
33 4.176	84 41.130	17.002	53592	53628
33 4.190	84 41.118	17.017	53595	53631
33 4.203	84 41.107	17.029	53591	53627
33 4.216	84 41.095	17.042	53593	53628
33 4.230	84 41.084	17.054	53610	53645
33 4.243	84 41.073	17.067	53589	53624
33 4.257	84 41.061	17.367	53605	53639
33 4.263	84 41.056	17.372	53602	53636
33 4.270	84 41.050	17.378	53604	53638
33 4.268	84 41.030	17.389	53593	53627
33 4.266	84 41.010	17.401	53585	53619
33 4.264	84 40.990	17.412	53506	53540
33 4.262	84 40.970	17.424	53595	53629
33 4.260	84 40.950	17.435	53594	53632
33 4.258	84 40.930	17.446	53605	53639
33 4.256	84 40.910	17.458	53594	53628
33 4.254	84 40.890	17.469	53605	53639
33 4.252	84 40.870	17.481	53605	53639
33 4.250	84 40.850	17.492	53557	53591
33 4.255	84 40.832	17.504	53589	53623
33 4.260	84 40.814	17.515	53612	53646
33 4.265	84 40.796	17.526	53610	53652
33 4.270	84 40.779	17.538	53621	53655
33 4.275	84 40.761	17.549	53616	53650
33 4.280	84 40.743	17.561	53613	53647
33 4.285	84 40.725	17.572	53614	53647
33 4.290	84 40.706	17.583	53609	53642
33 4.295	84 40.687	17.596	53608	53641
33 4.301	84 40.668	17.608	53615	53648
33 4.306	84 40.649	17.621	53622	53655
33 4.311	84 40.631	17.633	53626	53659
33 4.316	84 40.612	17.646	53624	53661
33 4.321	84 40.593	17.658	53624	53657
33 4.326	84 40.574	17.671	53629	53662
33 4.332	84 40.555	17.683	53624	53657
33 4.337	84 40.536	17.696	53654	53688
33 4.342	84 40.517	17.708	53651	53685
33 4.347	84 40.498	17.721	53636	53670
33 4.352	84 40.479	17.733	53667	53701
33 4.355	84 40.470	17.741	53695	53729
33 4.357	84 40.460	17.749	53768	53802
33 4.358	84 40.449	17.757	53631	53665
33 4.360	84 40.439	17.764	53644	53678
33 4.363	84 40.418	17.780	53657	53691
33 4.367	84 40.397	17.796	53689	53723
33 4.368	84 40.387	17.803	53734	53768
33 4.370	84 40.377	17.811	53732	53766
33 4.372	84 40.366	17.819	53650	53684
33 4.373	84 40.356	17.827	53673	53707
33 4.375	84 40.346	17.834	53655	53689
33 4.377	84 40.335	17.842	53659	53693
33 4.378	84 40.325	17.850	53666	53700
33 4.382	84 40.304	17.864	53676	53710
33 4.385	84 40.283	17.877	53707	53741
33 4.388	84 40.263	17.891	53719	53753
33 4.392	84 40.242	17.905	53749	53783
33 4.393	84 40.231	17.912	53784	53818
33 4.395	84 40.221	17.919	53852	53886
33 4.397	84 40.211	17.925	53849	53883
33 4.398	84 40.200	17.932	53922	53956
33 4.400	84 40.190	17.939	53965	53999
33 4.403	84 40.181	17.946	54111	54145
33 4.407	84 40.171	17.953	54592	54626
33 4.410	84 40.162	17.960	54246	54280
1234567890123456789012345678901234567890				

1234567890123456789012345678901234567890

Table 4. (Continued)

Profile A-A' (Concluded)

LATITUDE	LONGITUDE	TIME	RAW	REDUCED
1234567890123456789012345678901234567890				
33 4.875	84 39.190	18.680	53549	53581
33 4.875	84 39.170	18.700	53564	53596
33 4.875	84 39.150	18.713	53611	53644
33 4.875	84 39.130	18.725	53614	53647
33 4.875	84 39.110	18.738	53583	53616
33 4.875	84 39.090	18.750	53588	53621
33 4.875	84 39.070	18.763	53584	53617
33 4.875	84 39.050	18.776	53594	53627
33 4.875	84 39.030	18.788	53571	53603
33 4.875	84 39.010	18.801	53565	53597
33 4.875	84 38.990	18.813	53557	53589
33 4.875	84 38.980	18.820	53612	53644
33 4.875	84 38.970	18.826	53701	53732
33 4.875	84 38.960	18.832	53587	53618
33 4.875	84 38.940	18.845	53637	53668
33 4.875	84 38.930	18.851	53602	53633
33 4.875	84 38.920	18.857	53822	53853
33 4.875	84 38.910	18.864	53697	53728
33 4.875	84 38.890	18.876	53610	53640
33 4.875	84 38.870	18.889	53716	53746
33 4.875	84 38.850	18.901	53559	53589
33 4.875	84 38.830	18.914	53847	53877
33 4.875	84 38.820	18.920	53770	53800
33 4.875	84 38.810	18.927	53852	53882
33 4.875	84 38.800	18.933	53760	53790
33 4.875	84 38.780	18.946	5369A	53728
33 4.875	84 38.760	18.958	53920	53950
33 4.875	84 38.740	18.971	53680	53710
33 4.875	84 38.720	18.983	53576	53605
33 4.875	84 38.700	18.994	5354A	53577
33 4.875	84 38.680	19.006	53572	53601
33 4.875	84 38.660	19.017	53610	53639
33 4.875	84 38.640	19.028	53640	53669
33 4.875	84 38.620	19.039	53624	53653
33 4.875	84 38.600	19.050	53617	53646
33 4.875	84 38.580	19.061	53616	53645
33 4.875	84 38.560	19.072	53635	53664
33 4.875	84 38.540	19.083	53668	53697
33 4.875	84 38.520	19.094	53654	53683
33 4.875	84 38.500	19.106	53594	53623
33 4.875	84 38.480	19.117	53670	53699
33 4.875	84 38.460	19.131	53640	53669
33 4.875	84 38.440	19.144	53628	53657
33 4.875	84 38.420	19.158	53628	53657
33 4.875	84 38.400	19.172	53623	53652
33 4.875	84 38.380	19.186	53645	53674
33 4.875	84 38.360	19.200	53677	53706
33 4.875	84 38.340	19.212	53643	53672
33 4.875	84 38.320	19.224	5360A	53637
33 4.875	84 38.300	19.236	53599	53628
33 4.875	84 38.280	19.248	5359A	53627
33 4.875	84 38.260	19.260	53605	53634
33 4.875	84 38.240	19.271	53605	53634
33 4.875	84 38.220	19.283	53592	53621
1234567890123456789012345678901234567890				

Table 4. (Continued)

Profile B-B', May 5, 1973

Page missing from thesis

Table 4. (Continued)

Profile B-B' (Concluded)

Table 4. (Continued)

Profile C-C', May 6, 1973

Table 4. (Continued)

Profile C-C' (Concluded)

LATITUDE	LONGITUDE	TIME	RAW	REDUCED
1234567890123456789012345678901234567890				
33 1.930	84 38.810	13.819	53735	53772
33 1.925	84 38.790	13.830	53723	53760
33 1.921	84 38.770	13.842	53623	53661
33 1.916	84 38.750	13.853	53712	53750
33 1.913	84 38.740	13.859	53670	53708
33 1.909	84 38.720	13.871	53724	53762
33 1.904	84 38.700	13.882	53729	53767
33 1.899	84 38.680	13.894	53722	53760
33 1.894	84 38.660	13.905	53773	53811
33 1.892	84 38.650	13.911	53823	53861
33 1.890	84 38.640	13.917	53791	53829
33 1.885	84 38.620	13.937	53660	53698
33 1.889	84 38.602	13.957	53826	53864
33 1.890	84 38.593	13.967	53803	53842
33 1.892	84 38.584	13.977	53754	53793
33 1.894	84 38.575	13.987	53809	53849
33 1.896	84 38.566	13.997	53793	53833
33 1.899	84 38.548	14.017	53735	53776
33 1.903	84 38.530	14.027	53808	53849
33 1.906	84 38.512	14.038	53848	53889
33 1.910	84 38.494	14.049	53857	53899
33 1.913	84 38.476	14.060	53773	53A15
33 1.917	84 38.458	14.071	53783	53A25
33 1.920	84 38.440	14.081	53661	53703
33 1.920	84 38.421	14.092	53708	53751
33 1.920	84 38.403	14.103	53609	53652
33 1.919	84 38.384	14.114	53649	53692
33 1.919	84 38.365	14.125	53662	53705
33 1.919	84 38.347	14.135	53730	53773
33 1.919	84 38.328	14.146	53720	53764
33 1.918	84 38.309	14.157	53801	53845
33 1.918	84 38.291	14.168	53735	53779
33 1.918	84 38.272	14.178	53702	53746
33 1.918	84 38.253	14.189	53623	53667
33 1.918	84 38.235	14.200	53590	53634
33 1.917	84 38.216	14.210	53586	53631
33 1.917	84 38.197	14.221	53596	53642
33 1.917	84 38.179	14.231	53636	53682
33 1.917	84 38.160	14.241	53653	53700
33 1.916	84 38.141	14.251	53669	53716
33 1.916	84 38.123	14.262	53646	53693
33 1.916	84 38.113	14.267	53593	53640
33 1.916	84 38.095	14.277	53586	53633
33 1.916	84 38.076	14.287	53578	53625
33 1.915	84 38.057	14.297	53578	53625
33 1.915	84 38.039	14.308	53563	53610
33 1.915	84 38.020	14.318	53603	53650
33 1.915	84 38.010	14.323	53593	53640
33 1.915	84 37.991	14.333	53669	53717
33 1.915	84 37.972	14.344	53663	53711
33 1.914	84 37.953	14.355	53683	53731
33 1.914	84 37.934	14.365	53679	53727
33 1.914	84 37.915	14.376	53653	53701
33 1.914	84 37.886	14.392	53616	53664
33 1.914	84 37.867	14.403	53641	53689
33 1.914	84 37.847	14.413	53661	53712
33 1.913	84 37.828	14.424	53661	53710
33 1.913	84 37.809	14.435	53670	53719
33 1.913	84 37.790	14.445	53633	53682
33 1.913	84 37.771	14.456	53633	53682
33 1.913	84 37.751	14.467	53620	53669
33 1.913	84 37.732	14.477	53599	53648
33 1.912	84 37.713	14.488	53632	53681
33 1.912	84 37.694	14.499	53679	53729
33 1.912	84 37.675	14.509	53626	53676
1234567890123456789012345678901234567890				

LATITUDE	LONGITUDE	TIME	RAW	REDUCED
1234567890123456789012345678901234567890				
33 1.912	84 37.656	14.520	5363A	53688
33 1.912	84 37.636	14.531	5371n	53760
33 1.912	84 37.617	14.541	53676	53726
33 1.911	84 37.598	14.552	53779	53A29
33 1.911	84 37.579	14.563	5366A	53718
33 1.911	84 37.560	14.573	53651	53701
33 1.911	84 37.540	14.584	53619	53669
33 1.911	84 37.521	14.595	53614	53663
33 1.911	84 37.512	14.600	53614	53663
33 1.910	84 37.493	14.608	53609	53658
33 1.910	84 37.473	14.617	5361A	53667
33 1.910	84 37.454	14.625	53614	53663
33 1.910	84 37.435	14.633	53567	53616
1234567890123456789012345678901234567890				

Table 4. (Concluded)

Profile A'-B', May 6, 1973

LATITUDE	LONGITUDE	TIME	RAW	REDUCED
1234567890123456789012345678901234567890	1234567890123456789012345678901234567890	1234567890123456789012345678901234567890	1234567890123456789012345678901234567890	1234567890123456789012345678901234567890
33 4.875	84 38.740	10.033	53999	54014
33 4.859	84 38.735	10.045	54025	54040
33 4.843	84 38.731	10.056	54055	54070
33 4.827	84 38.726	10.068	54026	54041
33 4.811	84 38.721	10.079	53958	53973
33 4.796	84 38.716	10.090	53807	53822
33 4.780	84 38.712	10.102	53841	53856
33 4.764	84 38.707	10.113	53865	53880
33 4.748	84 38.702	10.125	53694	53709
33 4.740	84 38.700	10.130	53729	53737
33 4.724	84 38.700	10.142	53609	53625
33 4.707	84 38.700	10.153	53622	53638
33 4.691	84 38.700	10.164	5351n	53526
33 4.675	84 38.700	10.176	53679	53695
33 4.658	84 38.700	10.187	53614	53630
33 4.642	84 38.700	10.199	53625	53641
33 4.626	84 38.700	10.210	53658	53674
33 4.609	84 38.700	10.221	53681	53697
33 4.593	84 38.700	10.233	53761	53776
33 4.585	84 38.700	10.239	53644	53659
33 4.570	84 38.705	10.250	53593	53608
33 4.555	84 38.710	10.261	53526	53541
33 4.539	84 38.714	10.272	53630	53645
33 4.524	84 38.719	10.283	53589	53604
33 4.509	84 38.724	10.294	53589	53604
33 4.494	84 38.729	10.306	53589	53604
33 4.479	84 38.734	10.317	53592	53608
33 4.464	84 38.739	10.328	53595	53611
33 4.448	84 38.743	10.339	53593	53610
33 4.433	84 38.748	10.350	53590	53607
33 4.418	84 38.753	10.364	53597	53614
33 4.403	84 38.758	10.378	53582	53599
33 4.388	84 38.763	10.392	53579	53596
33 4.373	84 38.768	10.406	53559	53576
33 4.365	84 38.770	10.412	53806	53A23
33 4.357	84 38.769	10.419	53599	53616
33 4.342	84 38.768	10.433	53602	53619
33 4.327	84 38.766	10.467	53613	53630
33 4.312	84 38.765	10.500	53585	53602
33 4.296	84 38.763	10.533	53592	53609
33 4.281	84 38.762	10.567	53582	53600
33 4.266	84 38.760	10.600	53585	53603
33 4.251	84 38.759	10.633	53588	53606
33 4.235	84 38.757	10.667	5358n	53596
33 4.220	84 38.756	10.700	53577	53593
33 4.205	84 38.754	10.712	53591	53607
33 4.190	84 38.752	10.724	53580	53596
33 4.174	84 38.751	10.736	53582	53598
33 4.159	84 38.749	10.748	53581	53597
33 4.144	84 38.748	10.761	53571	53588
33 4.129	84 38.746	10.773	5357A	53595
33 4.113	84 38.745	10.785	5358n	53597
33 4.098	84 38.743	10.797	53581	53598
33 4.083	84 38.742	10.809	53577	53594
33 4.068	84 38.740	10.821	53584	53601
33 4.052	84 38.739	10.833	53577	53594
33 4.037	84 38.737	10.852	53572	53589
33 4.022	84 38.736	10.870	53573	53590
33 4.007	84 38.734	10.889	5357n	53588
33 3.991	84 38.733	10.907	53569	53587
33 3.976	84 38.731	10.926	5357n	53587
33 3.961	84 38.730	10.944	5356A	53585
33 3.946	84 38.728	10.963	53562	53579
33 3.930	84 38.727	10.981	53564	53582
33 3.915	84 38.725	11.000	53566	53584
1234567890123456789012345678901234567890	1234567890123456789012345678901234567890	1234567890123456789012345678901234567890	1234567890123456789012345678901234567890	1234567890123456789012345678901234567890

APPENDIX III

COMPUTER PROGRAMS FOR GRAVITY AND MAGNETICS MODELING

A computer program was developed for computing the vertical gravity anomaly caused by a hypothetical two-dimensioned structure using the method of Talwani, Worzel, and Landisman (1959). A listing of the main program and subroutines necessary for line printer plotting is given in Table 5.

A computer program was developed for computing horizontal, vertical, and total magnetic anomalies due to induction, NRM or mixed magnetization using the method of Talwani and Heirtzler (1965). A listing of the main program and all referenced subroutines is given in Table 6.

Table 5. Two-Dimensional Gravity Modeling Program

```

1234567890123456789012345678901234567890123456789012345678901234567890
C GRAVITY PROFILING FOR 2-DIMENSIONAL STRUCTURES
C GRAVITY FOR 2-DIMENSIONAL STRUCTURES(AFTER-TALWANI,WORTZEL,LANDIS,M,N)
C INPUT(2I10,3F10.3) CARD NO. ONE
C LL=NO. OF POLYGONS, N=X=NO. OF GRAVITY VALUES, DX=SEPARATION OF
C GRAVITY VALUES, XO=POSITION OF FIRST GRAVITY VALUE, SCALE=PLOT
C SCALE-FOR DRAW
C IF SCALE=0, PROGRAM CALCULATES SCALE
C IF SCALE=1, NO GRAPH IS DRAWN
C INPUT(FREE FIELD) LL CARDS
C NXZ=NO.+1OF CORNERS OF POLYGON TAKEN CLOCKWISE, DRHO=DENSITY
C CONTRAST, X(I,J),Z(I,J)=COORDINATES OF CORNERS-JTH CORNER OF ITH
C POLYGON
C REPEAT SEQUENCE FOR ADDITIONAL PROFILES
C BLANK CARD AT END TO TERMINATE CALCULATION
      DIMENSION DRHO(50),X(50,20),Z(50,20),NN(50),XX(20),ZZ(20),GAL(500)
      DIMENSION A(80)
25 READ (5,900)A
900 FORMAT(80A1)
      READ (5,500) LL,NDX,Dx,XO  * SCALE
      WRITE(6,901)A
901 FORMAT(1H1,80A1,//)
      WRITE(6,503) LL,NDX,Dx,XO
503 FORMAT(1H ,2BH VERTICAL GRAVITY ANOMALY FOR 15° 9H POLYGONS/2X,
13H THE,I5,16H-GRAVITY VALUES,F10.4*19H-KM.APART. BEGIN AT,F10.4)
      IF(LL) 26,20,27
27 DO 100 I=1,LL
500 FORMAT(2I10,3F10.5)
      READ(5,501) NXZ,DRHO(I),(X(I,J),Z(I,J),J=1,NXZ)
      WRITE(6,502) NXZ,DRHO(I),(X(I,J),Z(I,J),J=1,NXZ)
501 FORMAT( )
502 FORMAT(16H NO OF POINTS = ,1I0,22H DENSITY DIFFERENCE = /(1X,1nF10
<.3/))
100 NN(I) = NXZ
      DO 101 I=1,LL
      NNI = NN(I)
      DO 101 J = 1,NNI
101 X(I,J) = X(I,J) -XO
      DO 102 I=1,NDX
      G=0.0
      DO 103 J=1,LL
      NNJ = NN(J)
      DO 104 K = 1,NNJ
      XX(K) = X(J,K)
104 ZZ(K)=Z(J,K)
      CALL TWLZ(NN(J),XX,ZZ,DRHO(J),GA)
103 G= G+GA
      GAL(I) = G
      DO 110 M=1,LL
      NNM = NN(M)
      DO 110 N = 1,NNM
110 X(M,N) = X(M,N)-DX
102 CONTINUE
      WRITE(6,505) (GAL(I),I=1,NDX)
505 FORMAT(1X//24H GRAVITY ANOMALY IN MGAL,(5F15.4))
ISC=SCALE
      IF(ISC.EQ.13) GO TO 25
      IF(SCALE) 130,131,130
131 CALL MXSCL(NDX,GAL,SCALE)
130 CALL DRW(NDX,1,GAL,SCALE)
      GO TO 25
26 STOP
END
1234567890123456789012345678901234567890123456789012345678901234567890

```

Table 5. (Concluded)

```

1234567890123456789012345678901234567890123456789012345678901234567890
      SUBROUTINE TWLZ(K1,XX,ZZ,DRHO,GA)
C USES METHOD OF TALWANI, WILKEL, AND LANDISMAN (JGR 1959 PP 49-59)
C TO GIVE GRAVITY ANOMALY AT X=0,Z=0. IN MGAL FOR TWO DIMENSIONED
C BODY IN VERTICAL PLANE DESCRIBED BY A POLYGON (IN KILOMETERS)
      DIMENSION XX(K1),ZZ(K1)
      PI = 3.141592654
      KK = K1-1
      GA = 0.0
      DO 100 K=1,KK
      K2 = K+1
      IF(XX(K)+ZZ(K2)-XX(K2)+ZZ(K)) .EQ. 30.100+30
100   IF(XX(K)-XX(K2)) .EQ. 85+20,85
      XZ = ((XX(K2)**2 + ZZ(K2)**2)/(XX(K)**2 + ZZ(K)**2))
      DG = 0.5*LOG(XZ)*XX(K)
      GO TO 99
85   IF(ZZ(K)-ZZ(K2)) .EQ. 235+72+235
72   DG = ZZ(K)*(ATAN2(ZZ(K2),XX(K2))-ATAN2(ZZ(K),XX(K)))
      GO TO 99
235  A = (XX(K2)-XX(K))/(ZZ(K2)-ZZ(K))
      B = (XX(K)+ZZ(K2) - XX(K2)+ZZ(K))/(ZZ(K2)-ZZ(K))
      IF(XX(K)) .EQ. 200+201,200
201   DG = (B/(1.+A*A))*(.5*LOG((XX(K2)*XX(K2)+ZZ(K2)*ZZ(K2))/(ZZ(K)*
      1. ZZ(K))) - A*(ATAN2(ZZ(K2),XX(K2))-PI/2.))
200   IF(XX(K2)) .EQ. 31+210,31
210   DG = (B/(1.+A*A))*(.5*LOG((ZZ(K2)+ZZ(K2))/(XX(K)*XX(K)+
      1. ZZ(K)*ZZ(K))) + A*(ATAN2(ZZ(K),XX(K))-PI/2.))
31   DG=LOG((XX(K2)*XX(K2)+ZZ(K2)*ZZ(K2))/(XX(K)*XX(K)+ZZ(K)*ZZ(K)))
      DG=(B/(1.0+A*A))*(0.5*D-A*(ATAN2(ZZ(K2),XX(K2))-ATAN2(ZZ(K),
      1XX(K))))
99   GA=(13.34) *DRHO*DG + GA
100  CONTINUE
      RETURN
      END

      SUBROUTINE MXSCL(N,A,AUX)
      DIMENSION A(N)
      AMAX = 0
      DO 26 I = 1,N
      IF (ABS(A(I))-AMAX) .EQ. 26,26,25
25   AMAX = ABS(A(I))
26   CONTINUE
      AN = LOG10(AMAX)
      IF(AN) .EQ. 17+18+19
17   NN = AN - 1
      GO TO 20
19   NN = AN
20   IA = AMAX/(10.**NN)
      IF(IA.LE.2) GO TO 14
      IF(IA.LE.5) GO TO 15
16   AMAX = 10.* (10.**NN)
18   RETURN
14   AMAX = 2.* (10.**NN)
      RETURN
15   AMAX = 5.* (10.**NN)
      RETURN
      END

      SUBROUTINE DRAW (INTOT, INC, F, SCALE)
C INTOT=TOTAL NUMBER OF POINTS IN F. F IS THE DATA (ONE DIMENSIONAL)
C TO BE PLOTTED. INC IS THE SAMPLE INTERVAL FOR PLOTTING F.
C SCALE IS THE AMPLITUDE OF ONE FULL SCALE DEFLECTION
      DIMENSION F(INTOT)
      DATA AA1/1H /,AA2/1H/,AA3/1H+
      WRITE(6,1011) SCALE,(I,I=1,10) , (AA2,M=1,21)
1011 FORMAT(1H1,E14.8,17H-M,ALS FULL SCALE/3X,2015/2X,22A5)
10   DO 1501 K = 1, INTOT, INC
      FK = 50.*F(K)/SCALE
      KI = FK/50
      KK = FK - KI*50.+50.5
      WRITE (6,511) AA2, (AA1,I=1,KK)+AA2
511  FORMAT (1X,110A1)
1501 CONTINUE
      RETURN
      END
1234567890123456789012345678901234567890123456789012345678901234567890

```

Table 6. Two-Dimensional Magnetics Modeling Program

Table 6. (Continued)

Table 6. (Continued)

Table 6. (Continued)

```

123456789012345678901234567890123456789012345678901234567890
    CALL SPLOT(NFPTS,FLDPT,WORK1,WORK2,V#0RK,FSCALE,REMMAG(I),
    * MAX,IEXP0,ITICKS)
C***PLOT HORIZONTAL ANOMALY FOR THIS POLYGON -- REMANENT + INDUCED
123 IF (PLINH) 124+125+124
124 FSCALE = 0.0
    CALL CONARY(HANMLY,I,1,WORK1,NFPTS)
    CALL CONARY(HANMLY,I,2,WORK2,NFPTS)
    CALL GRSCAL(NFPTS,WORK1,FSCALE,IEXP0+MAX)
    CALL GRSCAL(NFPTS,WORK2,FSCALE,IEXP0+MAX)
    CALL GRSCAL(NFPTS+HWOR,FSCALE,IEXP0+MAX)
    WRITE (6,9008) I
9008 FORMAT (1H1+39X,'HORIZONTAL ANOMALY FOR POLYGON NUMBER ',I2)
    CALL SPLOT(NFPTS,FLDPT,WORK1,WORK2+HWORK,FSCALE,REMMAG(I),
    * MAX,IEXP0,ITICKS)
C***PLOT TOTAL ANOMALY FOR THIS POLYGON -- REMANENT + INDUCED
125 IF (PLINUT) 126,130+126
126 FSCALE = 0.0
    CALL CONARY(TANMLY,I,1,WORK1,NFPTS)
    CALL CONARY(TANMLY,I,2,WORK2,NFPTS)
    CALL GRSCAL(NFPTS,WORK1,FSCALE,IEXP0+MAX)
    CALL GRSCAL(NFPTS,WORK2,FSCALE,IEXP0+MAX)
    CALL GRSCAL(NFPTS+TWORK,FSCALE,IEXP0+MAX)
    WRITE (6,9009) I
9009 FORMAT (1H1+44X,'TOTAL ANOMALY FOR POLYGON NUMBER ',I2)
    CALL SPLOT(NFPTS,FLDPT,WORK1,WORK2+TWORK,FSCALE,REMMAG(I),
    * MAX,IEXP0,ITICKS)
130 CONTINUE
C*****END OF INDIVIDUAL POLYGON OUTPUT SECTION*****
C*****BEGIN FIELD POINT SUMMATION SECTION*****
C***ZERO ALL FIELD POINT SUMMING ARRAYS.
DO 135 I = 1,NFPTS
    VIND(I) = 0.0
    VREM(I) = 0.0
    HIND(I) = 0.0
    HREM(I) = 0.0
    TIND(I) = 0.0
    TREM(I) = 0.0
135 CONTINUE
DO 140 I = 1,NFOLY
DO 137 J = 1,NFOLY
    VIND(I) = VIND(I) + VAJMLY(I,J,1)
    HIND(I) = HIND(I) + HAJMLY(I,J,1)
    TIND(I) = TIND(I) + TAJMLY(I,J,1)
    VREM(I) = VREM(I) + VAJMLY(I,J,2)
    HREM(I) = HREM(I) + HAJMLY(I,J,2)
137 TREM(I) = TREM(I) + TAJMLY(I,J,2)
    VTOT(I) = VIND(I) + VREM(I)
    HTOT(I) = HIND(I) + HREM(I)
    TTOT(I) = TIND(I) + TREM(I)
140 CONTINUE
C*****END FIELD POINT SUMMATION SECTION*****
C*****BEGIN COMPOSITE OUTPUT SECTION*****
C***PLOT COMPOSITION FOR VERTICAL ANOMALY DUE TO INDUCTION ONLY
IF (VCOMP) 145+153,145
145 FSCALE = 0.0
DO 150 I = 1,NPOLY
    CALL CONARY(VANML,Y,I,1,WORK1,NFPTS)
150 CALL GRSCAL(NFPTS,WORK1,FSCALE,IEXP0+MAX)
    CALL GRSCAL(NFPTS,VIND,FSCALE,IEXP0+MAX)
    WRITE (6,9010)
9010 FORMAT (1H1+40X,'VERTICAL ANOMALY DUE TO INDUCTION ONLY.')
    CALL CPLOT(NPOLY,NFPTS,FLDPT,VANML,Y,1,VIND,FSCALE+1,MAX,IEXP0,
    * ITICKS)
C***PLOT COMPOSITION FOR VERTICAL ANOMALY DUE TO REMANENCE ONLY.
153 IF (VCUMPR) 155+133,155
155 FSCALE = 0.0
DO 160 I = 1,NPOLY
    CALL CONARY(VANML,I,2,WORK1,NFPTS)
160 CALL GRSCAL(NFPTS,WORK1,FSCALE,IEXP0+MAX)
    CALL GRSCAL(NFPTS,VREM,FSCALE,IEXP0+MAX)
    WRITE (6,9011)
9011 FORMAT (1H1+40X,'VERTICAL ANOMALY DUE TO REMANENCE ONLY.')
    CALL CPLOT(NPOLY,NFPTS,FLDPT,VANML,Y,2,VREM,FSCALE+1,MAX,IEXP0,
1234567890123456789012345678901234567890123456789012345678901234567890

```

Table 6. (Continued)

```

1234567890123456789012345678901234567890123456789012345678901234567890
* ITICKS)
C***PLOT COMPOSITION FOR HORIZONTAL ANOMALY DUE TO INDUCTION ONLY
163 IF (HCMP1) 165-173,165
165 FSCALE = 0.0
DO 170 I = 1,NPOLY
CALL CONARY(HANMLY,I,1,WOR,1,NFPTS)
170 CALL GRSCAL(NFPTS,WORK1+FSCALE,IEXP0+MAX)
CALL GRSCAL(NFPTS,HIND+FSCALE,IEXP0+MAX)
WRITE (6,9012)
9012 FORMAT (1H1+40X,'HORIZONTAL ANOMALY DUE TO INDUCTION ONLY')
CALL CPLOT(NPOLY,NFPTS,FLDPT,HANMLY,1,HIND,FSCALE,2,MAX,IEXP0,
* ITICKS)
C***PLOT COMPOSITION FOR HORIZONTAL ANOMALY DUE TO REMANENCE ONLY
173 IF (HCMPR) 175-183,175
175 FSCALE = 0.0
DO 180 I = 1,NPOLY
CALL CONARY(HANMLY,I,2,WOR,1,NFPTS)
180 CALL GRSCAL(NFPTS,WORK1+FSCALE,IEXP0+MAX)
CALL GRSCAL(NFPTS,HREM+FSCALE,IEXP0+MAX)
WRITE (6,9013)
9013 FORMAT (1H1+40X,'HORIZONTAL ANOMALY DUE TO REMANENCE ONLY')
CALL CPLOT(NPOLY,NFPTS,FLDPT,HANMLY,2,HREM,FSCALE,2,MAX,IEXP0,
* ITICKS)
C***PLOT COMPOSITION FOR TOTAL ANOMALY DUE TO INDUCTION ONLY
183 IF (TCMPI) 185-193,185
185 FSCALE = 0.0
DO 190 I = 1,NPOLY
CALL CONARY(TANMLY,I,1,WOR,1,NFPTS)
190 CALL GRSCAL(NFPTS,WORK1+FSCALE,IEXP0+MAX)
CALL GRSCAL(NFPTS,TIND+FSCALE,IEXP0+MAX)
WRITE (6,9014)
9014 FORMAT (1H1+40X,'TOTAL ANOMALY DUE TO INDUCTION ONLY')
CALL CPLOT(NPOLY,NFPTS,FLDPT,TANMLY,1,TIND,FSCALE,3,MAX,IEXP0,
* ITICKS)
C***PLOT COMPOSITION FOR TOTAL ANOMALY DUE TO REMANENCE ONLY
193 IF (TCOMPR) 195-205,195
195 FSCALE = 0.0
DO 200 I = 1,NPOLY
CALL CONARY(TANMLY,I,2,WOR,1,NFPTS)
200 CALL GRSCAL(NFPTS,WORK1+FSCALE,IEXP0+MAX)
CALL GRSCAL(NFPTS,TREM+FSCALE,IEXP0+MAX)
WRITE (6,9015)
9015 FORMAT (1H1+40X,'TOTAL ANOMALY DUE TO REMANENCE ONLY')
CALL CPLOT(NPOLY,NFPTS,FLDPT,TANMLY,2,TREM,FSCALE,3,MAX,IEXP0,
* ITICKS)
205 CONTINUE
C**** END COMPOSITE OUTPUT SECTION*****
C**** PEGIN ANOMALIES DUE TO ALL POLYGONS OUTPUT SECTION ****
C***PRINT OUT ANOMALIES DUE TO ALL POLYGONS
IF (PRNTAL) 206-260,206
206 REMFLG = 0.0
DO 210 I = 1,NPOLY
210 REMFLG = REMFLG + REMMAG(I)
WRITE (6,9016) NPOLY
9016 FORMAT (1H1+'ANOMALIES DUE TO ALL ',I2,' POLYGON(S)')
IF (REMFLG) 230-220,230
220 WRITE (6,B000)
GO TO 240
230 WRITE (6,9017)
9017 FORMAT (1H1+'MAGNETIZATION IS MIXED.')
240 WRITE (6,9018)
DO 250 I = 1,NFPTS
250 WRITE (6,9012) FLDPT(I),VIND(I),HIND(I),TIND(I),VREM(I),HREM(I),
1 TREM(I),VTOT(I),HTOT(I),TTOT(I)
C*** PLOT VERTICAL ANOMALY DUE TO ALL POLYGONS -- REMANENT + INDUCED
260 IF (PLVAL) 270-281,270
270 FSCALE = 0.0
CALL GRSCAL(NFPTS,VIND+FSCALE,IEXP0+MAX)
CALL GRSCAL(NFPTS,VREM+FSCALE,IEXP0+MAX)
CALL GRSCAL(NFPTS,VTOT+FSCALE,IEXP0+MAX)
WRITE (6,9018)
9018 FORMAT (1H1+41X,'VERTICAL ANOMALY DUE TO ALL POLYGONS')
CALL SPLOT (NFPTS,FLDPT,VI+VIND,VTOT,FSCALE,REMFLG+MAX,IEXP0,
1234567890123456789012345678901234567890123456789012345678901234567890

```

Table 6. (Continued)

```

1234567890123456789012345678901234567890123456789012345678901234567890
* ITICKS)
C****+*****+PLOT HORIZONTAL ANOMALY DUE TO ALL POLYGONS - REMANENT + INDUCED
28n IF (PLHAL) 290,300,290
290 FSCALE = 0.0
CALL GRSCAL(NFPTS,HIIND,FSCALE,IEXPO,MAX)
CALL GRSCAL(NFPTS,HKEM,FSCALE,IEXPO,MAX)
CALL GRSCAL(NFPTS,HTOT,FSCALE,IEXPO,MAX)
WRITE (6,9019)
9019 FORMAT (1H1,41X,'HOKIZ-N.TAI ANOMALY DUE TO ALL POLYGONS')
CALL SPLUT (NFPTS,FLOPT,HIIND,HTOT,FSCALE,REMFLG,MAX,IEXPO,
* ITICKS)
C****+*****+PLOT TOTAL ANOMALY DUE TO ALL POLYGONS- REMANENT + INDUCED
30n IF (PLTAL) 310,315,310
310 FSCALE = 0.0
CALL GRSCAL(NFPTS,TIND,FSCALE,IEXPO,MAX)
CALL GRSCAL(NFPTS,TREM,FSCALE,IEXPO,MAX)
CALL GRSCAL(NFPTS,TTOT,FSCALE,IEXPO,MAX)
WRITE (6,9020)
9020 FORMAT (1H1,45X,'TOTAL ANOMALY DUE TO ALL POLYGONS')
CALL SPLUT (NFPTS,FLOPT,TIND,TREM,TTOT,FSCALE,REMFLG,MAX,IEXPO,
* ITICKS)
315 GO TO 1
320 CALL EXIT
END
1234567890123456789012345678901234567890123456789012345678901234567890

```

```

1234567890123456789012345678901234567890123456789012345678901234567890
SUBROUTINE GRSCAL(NFPTS,A,FSCALE,IEXPO,MAX)
DIMENSION A(200)
C****+*****+*****+*****+*****+*****+*****+*****+*****+*****+*****+*****+*****
C THIS SUBROUTINE FINDS THE VARIABLE WITH THE GREATEST ABSOLUTE VALUE IN THE
C ARRAY A WHICH HAS NFPTS ELEMENTS.
C FSCALE IS THEN SET EQUAL TO THE SMALLEST VALUE FOR FULL SCALE WHICH WILL
C BEST PRESENT THE ELEMENTS OF A.
C IEXPO AND MAX ARE SUCH THAT FSCALE = MAX * 10 ** IEXPO .
C****+*****+*****+*****+*****+*****+*****+*****+*****+*****+*****+*****
DO 15 I = 1,NFPTS
5 IF (ABS(A(I))=FSCALE) 15,15,10
10 FSCALE = ABS(A(I))
15 CONTINUE
C** IF ALL VALUES OF THE ARRAY ARE ZERO SET FSCALE = 1.0 ARBITRARILY.
IF (FSCALE) 20,20,25
20 FSCALE = 1.0
25 EXPO = LOG10 (FSCALE)
IF (EXPO) 30,35,40
30 IEXPO = EXPO + 1
GO TO 45
35 MAX = 1
RETURN
40 IEXPO = EXPO
45 J = FSCALE/(10.0**IEXPO)
IF (J.LT.2) GO TO 50
IF (J.LT.5) GO TO 55
FSCALE = 10.0 * (10.0**IEXPO)
MAX = 10
RETURN
50 FSCALE = 2.0 * (10.0**IEXPO)
MAX = 2
RETURN
55 FSCALE = 5.0 * (10.0**IEXPO)
MAX = 5
RETURN
END
1234567890123456789012345678901234567890123456789012345678901234567890

```

Table 6. (Continued)

```

1234567890123456789012345678901234567890123456789012345678901234567890
      SU,ROUTINE POLYPO (NFPTS,NSIDES,FLOPT,OBSVHT,PSUM,GSUM,
      * INDEX,X,Z,DELX)
      DIMENSION FXX(21),ZEE(1),FLOPT(200),PSUM(200),GSUM(200)
      DIMENSION X(1:20),Z(1:20)
*****
C***READ COORDINATE CARDS FOR POLYGON CORNERS
C***ONE COORDINATE CARD FOR EACH CORNER OF THE POLYGON--CLOCKWISE ORDER.
C***FXX(I) = X COORDINATE OF THE ITH CORNER OF POLYGON
C***ZEE(I) = Z COORDINATE OF THE ITH CORNER OF POLYGON. POSITIVE DOWN.
C***SAVE CORNER COORDINATES FOR PRINTOUT.
      DO 10 I = 1,NSIDES
      READ (5,1000) EXX(I),ZEE(I)
1000 FORMAT( )
      X(INDEX,I) = EXX(I)
      10 Z(INDEX,I) = ZEE(I)
      NSIDUP1 = NSIDES + 1
      EXX(NSIDUP1) = EXX(1)
      ZEE(NSIDUP1) = ZEE(1)
      DO 150 I = 1,NFPTS
      PSUM(I) = 0.0
      GSUM(I) = 0.0
      X1 = EXX(1) - FLOPT(1)
      Z1 = ZEE(1) + OBSVHT
15  RSQ1 = (X1*X1+Z1*Z1)
C***IF X AND Z ARE BOTH ZERO, ATAN2 GIVES ERROR, SO CHANGE Z SLIGHTLY
      IF (RSQ1.NE.0.0) GO TO 17
      Z1 = .0001 * DELX
      THETD = 0.0
      GL = ALOG (.0001 * DELX * DELX)
      GO TO 15
17  THETA = ATAN2(Z1,X1)
      J = 2
20  X2 = EXX(J) - FLOPT(1)
      Z2 = ZEE(J) + OBSVHT
25  RSQ2 = (X2*X2+Z2*Z2)
      IF (RSQ2.NE.0.0) GO TO 27
      Z2 = .0001 * DELX
      THETD = 0.0
      GL = ALOG (.0001 * DELX * DELX)
      GO TO 25
27  THETB = ATAN2(Z2,X2)
      IF (Z1-Z2) 40,30,40
30  P = 0.0
      Q = 0.0
      GO TO 120
40  OMEGA = THETA - THETB
      IF (OMEGA) 60,50,50
50  IF (OMEGA-3.1415927) 70,70,A0
60  IF (OMEGA+3.1415927) 30,70,70
70  THETU = OMEGA
      GO TO 110
80  IF (OMEGA) 90,100,100
90  THETU = OMEGA - 6.283153
      GO TO 110
100 THETD = OMEGA + 6.283153
110 GL = 0.5 * ALOG(RSQ2/RSQ1)
115 X12 = X1 - X2
      Z21 = Z2 - Z1
      XSQ = X12 * X12
      ZSQ = Z21 * Z21
      XZ = Z21 * X12
      P = -(ZSQ/(XSQ+ZSQ)) * THETD + ((XZ/(XSQ+ZSQ)) * GL)
      Q = -(THETD*(XZ/(XSQ+ZSQ))) - (GL*(ZSQ/(XSQ+ZSQ)))
120 PSUM(1) = PSUM(1) + P
      GSUM(1) = GSUM(1) + Q
C***RELATIONAL VARIABLES INVOLVING ONLY THE SECOND POLYGON CORNER AS THE
C*** VARIABLFS INVOLVING ONLY THE FIRST POLYGON CORNER SO THEY DON'T
C*** HAVE TO BE CALCULATED AGAIN.
140 X1 = X2
      Z1 = Z2
      RSQ1 = RSQ2
      THETA = THETB
1234567890123456789012345678901234567890123456789012345678901234567890

```

Table 6. (Continued)

```

1234567890123456789012345678 01234567890123456789012345678901234567890
C***CHECK TO SEE IF ALL SIDES HAVE BEEN DONE.
      J = J + 1
      JR = J - 1
      IF(JR-.SIDP1) 20+150+150
150 CONTINUE
      RETURN
      END
1234567890123456789012345678901234567890123456789012345678901234567890

1234567890123456789012345678901234567890123456789012345678901234567890
SUBROUTINE CONAHY (ARR1,I,J,ARRAY2,NFPTS)
      DIMENSION ARRAY1(200,1NF2),ARRAY2(200)
C***** THIS SUBROUTINE SELECTS THE DESIGNATED ELEMENTS OF THE THREE DIMENSIONAL
C      ARRAY, ARRAY1 AND PUTS THEM INTO A ONE DIMENSIONAL ARRAY, ARRAY2)
C      THAT IS ARRAY2(1) = ARRAY1(1,I,J) THRU TO
C      ARRAY2(NFPTS) = ARRAY1(NFPTS,I,J) ARE PERFORMED.
C*****
      DO 10 K = 1,NFPTS
10  ARRAY2(K) = ARRAY1(K,I,J)
      RETURN
      END
1234567890123456789012345678901234567890123456789012345678901234567890

```

Table 6. (Continued)

```

1234567890123456789012345678901234567890123456789012345678901234567890
      SU,ROUTINE SPLOT (NFPTS,FLDPT,A*,C,FSCALE,REMFLG,MAX,IEXPO,
      * ITICKS)
      DIMENSION A(200),B(200),C(200),FLDPT(200),ALINE(101)
      REAL II
      DATA BLNK/1H /*AST/1H*/,*DOT/1H/,RR/IHR/,II/IHT/,DASH/1H-/,PLS/1H+
***** ****,***** ****,***** ****,***** ****,***** ****,***** ****,*****
C THIS SUBROUTINE GENERATES A LINE PRINTER PLOT OF THE ELEMENTS OF THE ARRAYS
C A , B & C VS. THE FIELD P(I,TS), FLDPT .
C FLDPT ELEMENTS ARE LISTED ALONG THE ABSCISSA AND THE ARRAY ELEMENTS
C PLOTTED ALONG THE ODUINATE. HATCH MARKS ARE PLACED ALONG THE ABSCISSA
C EVERY ITICKS TH POINT.
C FSCALE IS THE FULL SCALE LIMIT OF THE PLOT.
C FSCALE = MAX * 10 ** IEXPO
C REMFLAG PERMITS CHOICE OF PLOTTING SYMBOLS DEPENDING ON WHETHER THE MAG-
C NETIZATION IS MIXED OR NOT.
C REMFLAG 0 , USE SYMBOLS FOR INDUCTION ONLY
C = 1 , USE SYMBOLS FOR MIXED MAGNETIZATION
***** ****,***** ****,***** ****,***** ****,***** ****,***** ****,*****
      N = ITICKS
      WRITE (6,500) IEXPO,IE,PO,AX,MAX
500 FORMAT (1H+,17X,I1.99X,I1,/-12X,-I2,1X10',47X,'0',46X,'+',1
     1 I2,1X10',/, FIELD POINT',3X,21('' '' ),/15X,21(5H'   '))
      WRITE (6,600)
600 FORMAT (1H+,14X,20('+' ,...'),'+')
      DO 10 I = 1,101
10 ALINE(I) = BLNK
      ALINE( 1) = DOT
      ALINE( 51) = DOT
      ALINE(101) = DOT
      DO 30 I = 1,NFPTS
      IF (ITICKS-N) 13,12,13
12 N = 1
      ALINE( 1) = PLS
      ALINE( 2) = DASH
      ALINE( 50) = DASH
      ALINE( 51) = PLS
      ALINE( 52) = DASH
      ALINE(100) = DASH
      ALINE(101) = PLS
      GO TO 14
13 N = N + 1
14 J = 51.500001 + (A(I)/FSCALE)*50
      M = IFIX (1000.0 * REMFLG)
      IF (M) 16,15,16
15 ALINE(J) = AST
      L = J
      K = J
      GO TO 18
16 ALINE(J) = II
      K = 51.500001 + (B(I)/FSCALE)*50+0
      ALINE(K) = RR
      L = 51.500001 + (C(I)/FSCALE)*50+0
      ALINE(L) = AST
18 WRITE (6,1000) FLDPT(I),ALINE
1000 FORMAT (1H ,F10.2,4X,101A1)
      WRITE (6,2000)
2000 FORMAT (1H+,14X,1H*,99X,1H*)
      IF (N-1) 25,20,25
20 ALINE ( 2) = BLNK
      ALINE ( 50) = BLNK
      ALINE ( 52) = BLNK
      ALINE (100) = BLNK
25 ALINE(L) = BLNK
      ALINE(K) = BLNK
      ALINE(J) = BLNK
      ALINE( 1) = DOT
      ALINE( 51) = DOT
      ALINE(101) = DOT
30 CONTINUE
      WRITE (6,3000)
3000 FORMAT (1H+,14X,20('+' ,...'),'+')
      RETURN
      END
1234567890123456789012345678901234567890123456789012345678901234567890

```

Table 6. (Concluded)

```

12345678901234567890123456789012345678901234567890123456789012345678901234567890
      SUBROUTINE CPLOT(NPOLY,NFPTS,FLDPT,A,K,R,FSCALE,INDEX,MAX,IEXPO,
      * ITICKS)
      DIMENSION FLDPT(200),A(200,10,2),B(200),ALINE(101),SUM(3),LINE(11)
      REAL NUM(10)
      DATA BLNK/1H //DOT/1H.,/(NUM(I),I=1,10)/1H1,1H2,1H3,1H4,1H5,1H6,
      * 1H7,1H8,1H9,1H0/, (SU(I),I=1,3)/1HV,1HH,1HT//DASH/1H-/,PLS/1H+/
C THIS SUBROUTINE GENERATES A COMPOSITE LINE PRINTER PLOT OF THE ELEMENTS OF
C THE ARRAY A AS FOLLOW. NOTE A IS DIMENSIONED AS A(200,10,2).
C THIS SUBROUTINE WILL PLOT THE POINTS A(ALPHA,BETA,1) OR
C A(ALPHA,BETA,2) AS DESCRIBED BY THE FOLLOWING. NPOLY PLOTTING SYMBOLS
C ARE PLOTTED FOR EACH VALUE OF THE ABSISSA, FOR NFPTS FIELD POINTS. ALSO
C FOR EACH VALUE OF THE ABSISSA A PLOTTING SYMBOL REPRESENTING THE CORRESPOND-
C ING ELEMENT OF THE ARRAY B , WHICH IN THIS CASE REPRESENTS THE ALGEBRAIC
C SUM OF THE NPOLY VALUES FOR ARRAY A IS ALSO PLOTTED.
C FLPT ELEMENTS ARE LISTED ALONG THE ABSISSA AND THE ARRAY ELEMENTS OF
C A AND B ARE PLOTTED ALONG THE ORDINATE. HATCH MARKS ARE PLACED ALONG
C THE ABSISSA EVERY ITICKS TH POINT. FSCALE IS THE FULL SCALE LIMIT OF
C THE PLOT. FSCALE = MAX + 10 ** IEXPO .
      N = ITICKS
      WRITE (6,500) IEXPO,IE,P0,MAX,MAX
500 FORMAT (1H+17X,11.99X,11,/-1,I2, X10',47X,'0',46X,'+',1
      12,'X10',// FIELD POINT',3X,21(' ',     ' ),/15X,21(5H'   '))
      WRITE (6,600)
600 FORMAT (1H+,14X,20('+'....'),'+')
      DO 10 I = 1,101
      10 ALINE(I) = BLNK
      ALINE( 1) = DOT
      ALINE( 51) = DOT
      ALINE(101) = DOT
      DO 40 I = 1,NFPTS
      IF (ITICKS-N) 13,12,13
      12 N = 1
      ALINE( 1) = PLS
      ALINE( 2) = DASH
      ALINE( 50) = DASH
      ALINE( 51) = PLS
      ALINE( 52) = DASH
      ALINE(100) = DASH
      ALINE(101) = PLS
      GO TO 14
      13 N = N + 1
      14 DO 20 J = 1,NPOLY
      L = 51.500001 + (A(I,J,K)/FSCALE) * 50.0
C***SAVE NUMBER OF THE ELEMENT WHICH WAS CHANGED FROM BLANK
      LINE(J) = L
C***REPLACE BLANK LINE ELEMENT BY CHARACTER FOR DATA POINT.
      20 ALINE(L) = NUM(J)
      L = 51.500001 + (B(I)/FSCALE) * 50.0
      ALINE(L) = SUM(INDEX)
C***J IS NOW = NPOLY + 1
      LINE(J) = L
      WRITE(6,1000) FLDPT(I),ALINE
1000 FORMAT(1H ,F10.2,4X,101A1)
      WRITE (6,2000)
2000 FORMAT (1H+,14X,1H',99X,1H+)
C***RESTORE BLANKS TO THOSE LINE ELEMENTS WHICH WERE CHANGED
      DO 30 L = 1,J
      M = LINE(L)
      30 ALINE(M) = BLNK
C***RESTORE DOTS TO THOSE LINE ELEMENTS WHICH MAKE UP THE AXIS AND M,Y HAVE
C*** BEEN CHANGED.
      IF (N-1) 38,35,38
      35 ALINE( 2) = BLNK
      ALINE( 50) = BLNK
      ALINE( 52) = BLNK
      ALINE(100) = BLNK
      38 ALINE( 1) = DOT
      ALINE( 51) = DOT
      ALINE(101) = DOT
      40 CONTINUE
      WRITE (6,3000)
3000 FORMAT (1H+14X,20('+'....'),'+')
      RETURN
      END
12345678901234567890123456789012345678901234567890123456789012345678901234567890

```

APPENDIX IV

PALEOMAGNETIC DATA COLLECTION AND REDUCTION

Samples from the Meriwether dike were collected and analyzed for NRM (Natural Remanent Magnetization) by Doyle Watts of the Ohio State University. Thirteen cores were obtained from a single outcrop of the Meriwether dike 5.5 miles northeast of Greenville on Georgia State Highway 362. In all, 26 one inch cylinders were cut from the cores. The samples were analyzed for Natural Remanent Moment (no magnetic cleaning) using a Schonstedt SSML Spinner Magnetometer. Direction and magnitude of the NRM are given for each sample in Table 7. Sample numbers are those used by Watts (personal communication) and the letter A, B, or C following the number indicates the first, second, or third cylinder cut from a core. Cores NW73174 through NW73182 were taken from the center portion of the dike and the remaining cores from the chilled edges of the dike.

Table 7. Natural Remanent Moments of Cores Taken From
The Meriwether Dike (Watts, Personal Communication)

Ohio State University Sample Number	Remanent Moment		
	Magnitude	Declination	Inclination
NW73174B	0.00144	7.82	26.26
NW73175A	0.00144	2.98	28.54
NW73175B	0.00156	8.86	35.49
NW73176B	0.00150	1.03	35.39
NW73177B	0.00150	21.69	27.86
NW73177C	0.00151	18.31	35.96
NW73178B	0.00174	12.42	25.20
NW73178C	0.00168	13.94	26.29
NW73179B	0.00152	18.10	22.61
NW73179C	0.00149	22.29	21.84
NW73180B	0.00173	10.08	26.39
NW73180C	0.00175	14.89	25.46
NW73180D	0.00170	12.01	27.20
NW73181B	0.00166	14.77	29.96
NW73182B	0.00162	16.20	23.21
NW73182C	0.00153	19.51	25.58
NW73183B	0.00215	36.16	27.72
NW73183C	0.00220	36.84	31.15
NW73184B	0.00211	33.78	23.38
NW73184C	0.00173	30.42	16.23
NW73185B	0.00201	42.87	27.96
NW73185C	0.00193	46.15	27.09
NW73186B	0.00220	42.11	32.70
NW73186C	0.00210	46.66	31.44
NW73187B	0.00212	49.75	30.89
NW73187C	0.00216	42.37	30.95

BIBLIOGRAPHY

BIBLIOGRAPHY

- Armstrong, R.L., and J. Besancon. A triassic time scale dilemma: K-Ar dating of Upper Triassic mafic igneous rocks of eastern U.S.A. and Canada and Post-Upper Triassic plutons, western Idaho, U.S.A. *Eclogae geol. Helv.*, 63(1), 15-38, 1970.
- Balsley, J.R., and A.F. Buddington. Iron-Titanium Oxide minerals, rocks, and aeromagnetic anomalies of the Adirondack Area, New York. *Economic Geology*, 53, 777-805, 1958.
- Bentley, R.D., and T.L. Neathery. Geology of the Brevard zone and related rocks of the inner Piedmont of Alabama. *Alabama Geol. Survey, 8th Annual Field Trip Guidebook*, Dec. 4-5, 1970.
- Cohee, C.V., Chairman. Tectonic Map of the United States excluding Alaska and Hawaii. U.S. Geological Survey and American Association of Petroleum Geologists, scale 1:2,500,000, 1962.
- de Boer, Jelle. Paleomagnetic-tectonic study of Mesozoic dike swarms in the Appalachians. *J. Geophys. Res.*, 72(8), 2237-2250, 1967.
- Dobrin, M.B. Introduction to Geophysical Prospecting. Second edition, McGraw-Hill, 446 pages, 1960.
- Dorman, Leroy M., and Robert E. Ziegler. Gravimetric reference base net, State of Georgia. *Georgia Geological Survey*, in preparation.
- Garland, George D. Introduction to Geophysics - Mantle, Core, and Crust. Saunders, 420 pages, 1971.
- Georgia Department of Mines, Mining, and Geology. *Geologic Map of Georgia*, scale 1:500,000, 1939.
- Green, R. Remanent magnetization and the interpretation of magnetic anomalies. *Geophysical Prospecting*, 8, 98-110, 1960.
- Hood, Peter. Remanent magnetism - a neglected factor in aeromagnetic interpretation. *Canadian Mining Journal*, 84(4), 76-79, 1963.
- Johnson, Robert W., and Joel S. Watkins, Aeromagnetic map of Staunton and vicinity, Virginia. U.S. Geological Survey, *Geophysical Investigations Map GP-414*, scale 1:62,500, 1963.
- King, P.B. Systematic pattern of Triassic dikes in the Appalachian region. *Geological Survey Research 1961*, U.S. Geol. Survey Prof. Paper 424-B, B93-B95, 1961.

Lee, Doyce L. A diabase dike in Meriwether County, Georgia (abstr.) Bull. of the Ga. Acad. of Sci., 29(2), 127, 1971.

Lester, J.G., and A.T. Allen. Diabase of the Georgia Piedmont. Bull. of the Geol. Soc. of Amer., 61, 1217-1224, 1950.

Matshusita, S., and Wallace H. Campbell, editors. Physics of Geomagnetic Phenomena, Vol 1. Academic Press, 1967.

May, P.R. Pattern of Triassic-Jurassic diabase dikes around the North Atlantic in the context of predrift position of the continents. Geol. Soc. of Amer. Bull., 82, 1285-1292, 1971.

National Aeronautics and Space Administration. Earth Resources Aircraft Program, Screening and Indexing Report, Mission 131. Manned Spacecraft Center; Houston, Texas; September 1970. Film: Mission 131, site 217, roll 3, Color infrared Zeiss camera, frames 43, 44, and 45, 1970.

Petty, A.J., F.A. Petrafeso, and F.C. Moore, Jr. Aeromagnetic Map of the Savannah River Plant Area South Carolina and Georgia. U.S. Geological Survey, Geophysical Investigations Map GP-489, scale 1:250,000, 1965.

Philbin, P.W., F.A. Petrafeso, and C.L. Long. Aeromagnetic Map of the Georgia Nuclear Laboratory Area, Georgia. U.S. Geological Survey Geophysical Investigations Map GP-488, scale 1:250,000, 1964.

Privett, Donald R. Structure and petrography of some diabase dikes in central South Carolina (abstr.). Geol. Soc. Amer. Spec. Paper 87, p. 260, 1966.

Stockwell, C.H., Chairman. Tectonic Map of Canada. Canada Geological Survey, Map 1251A, scale 1:5,000,000, 1969.

Strangway, D.W. Interpretation of the magnetic anomalies over some Precambrian dikes. Geophysics, XXX(5), 783-796, 1965.

Talwani, Manik, J.L. Worzel, and Mark Landisman. Rapid gravity computations for two-dimensional bodies with application to the Mendocino submarine fracture zone. J. Geophys. Res., 64(1), 49-59, 1959.

Talwani, Manik, and James R. Heirtzler. Computation of magnetic anomalies caused by two-dimensional structures of arbitrary shape. Computers in the Mineral Industries, Part I, Stanford University Publications, Geol. Sci., 9(1), 464-480, 1965.

U.S. Geological Survey. North-Central Georgia Aeromagnetic Map. Georgia Geological Survey, in preparation.

Watson, Thomas L. Granites and gneisses of Georgia. Geological Survey of Georgia Bull. 9A, 1902.

Weigand, Peter W., and Paul C. Ragland, Geochemistry of Mesozoic dolerite dikes from eastern North America. Contr. Mineral and Petrol., 29, 195-214, 1970.